

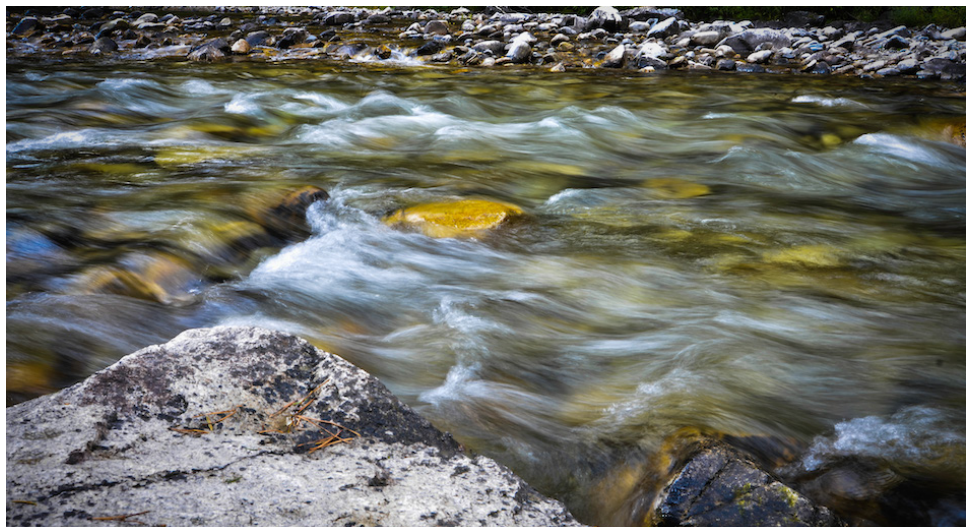
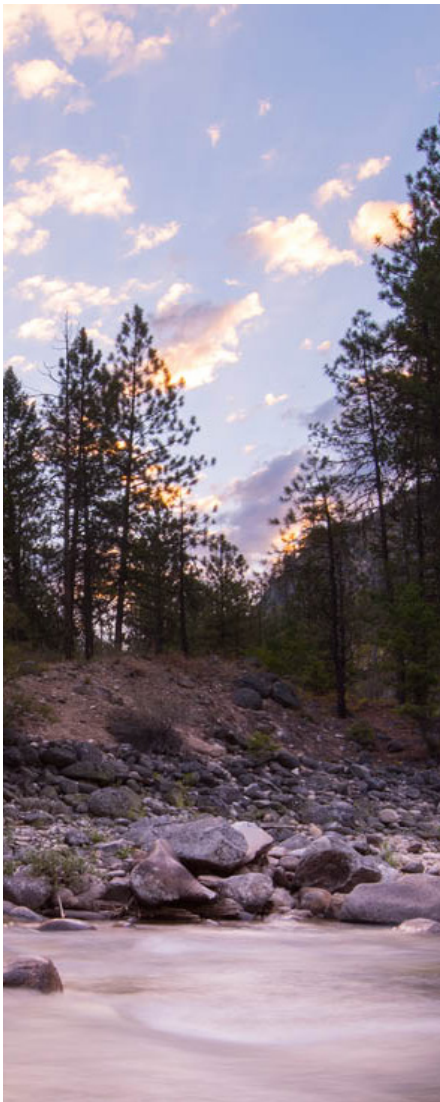
Prepared for
Midas Gold Idaho, Inc., Valley County, Idaho



Draft Stibnite Gold Project

Hydrologic Model Existing Conditions

November 15, 2017



DRAFT

Stibnite Gold Project Hydrologic Model Existing Conditions

Prepared for
Midas Gold Idaho, Inc., Valley County, Idaho
November 15, 2017

Bradley A. Hart, Idaho PG#937

This is a draft and is not intended to be a final representation
of the work done or recommendations made by Brown and Caldwell.
It should not be relied upon; consult the final report.



950 West Bannock Street, Suite 350
Boise, ID 83702
Phone: 208.389.7700
Fax: 208.389.7750

Table of Contents

List of Figures	ii
List of Graphs	iii
List of Tables	iv
List of Abbreviations	v
Executive Summary	ES-1
1. Introduction	1-1
1.1 Site Background and Project Plan	1-2
1.2 Report Organization	1-2
2. Hydrologic Setting and Conceptual Model	2-1
2.1 Climate	2-1
2.2 Surface Water Hydrology	2-2
2.3 Groundwater Hydrogeology	2-3
2.3.1 Groundwater Occurrence and Flow System Boundaries	2-3
2.3.2 Groundwater Data for Numerical Modeling	2-5
3. Meteoric Water Balance	3-1
4. Numerical Model Setup	4-1
4.1 Simulation Period	4-1
4.2 Model Discretization	4-1
4.3 Model Boundary Conditions	4-2
4.3.1 Recharge	4-2
4.3.2 Stream Flow	4-3
4.4 Aquifer Physical Parameters	4-5
5. Model Calibration	5-1
5.1 Seasonal Groundwater Fluctuations	5-1
5.2 Groundwater Levels	5-1
5.3 Surface Water Flows	5-3
5.4 Gestrin Well Test, December 2013	5-8
6. Discussion and Conclusions	6-1
7. References	7-1
8. Figures	8-1

List of Figures

Figure 1-1. Location Map of the Stibnite Gold Project, Valley County, Idaho

Figure 1-2. Proposed Stibnite Gold Project Mine Features	
Figure 2-1. EFSFSR Streams and Basins	
Figure 2-2. USGS Surface Flow Gaging Stations	
Figure 2-3. Groundwater Monitoring Locations	
Figure 2-4. Alluvial Groundwater Elevations and Contours—Fall 2015	
Figure 2-5. Thickness of Overburden	
Figure 3-1. Schematic Showing Modeling Structure	
Figure 4-1. Existing Conditions Model Lateral Extent	
Figure 4-2. Existing Conditions Model Grid	
Figure 4-3. Extent of Overburden Analysis	
Figure 4-4. Cross Section Through Model Row 130	
Figure 4-5. Cross Section Through Model Row 60	
Figure 4-6. Model Recharge Zones	
Figure 4-7. Simulated SFR Segments	
Figure 4-8. Model Layer 1 Hydraulic Conductivity	
Figure 4-9. Model Layer 2 Hydraulic Conductivity	
Figure 4-10. Model Layer 2 Specific Yield	
Figure 5-1. Simulated Water Table, December 2015	
Figure 5-2. Simulated Extent of Saturated Alluvium and Overburden, February 2015	
Figure 5-3. Simulated Extent of Saturated Alluvium and Overburden, July 2015	
Figure 6-1. Project Modeling Process Diagram	

List of Graphs

Graph 2-1. Flow in the EFSFSR at Stibnite (USGS 13311000), linear scale	2-3
Graph 3-1. Example of short-term monthly recharge estimates 1985–1990.....	3-3
Graph 3-2. Annual recharge estimates	3-3
Graph 3-3. Example of short-term monthly runoff estimates 1985–1990	3-4
Graph 3-4. Annual runoff estimates	3-4
Graph 5-1. Scatterplot showing simulated versus observed water levels	5-3
Graph 5-2. Measured vs. simulated flow at USGS gaging station 13310800, EFSFSR above Meadow Creek (linear)	5-4
Graph 5-3. Measured vs. simulated flow at USGS gaging station 13310800, EFSFSR above Meadow Creek (logarithmic)	5-4

Graph 5-4. Measured vs. simulated flow at USGS gaging station 13310850, Meadow Creek near Stibnite, ID (linear).....	5-5
Graph 5-5. Measured vs. simulated flow at USGS gaging station 13310850, Meadow Creek near Stibnite, ID (logarithmic)	5-5
Graph 5-6. Measured vs. simulated flow at USGS gaging station 13311000, EFSFSR at Stibnite (linear).....	5-6
Graph 5-7. Measured vs. simulated flow at USGS gaging station 13311000, EFSFSR at Stibnite (logarithmic).....	5-6
Graph 5-8. Measured vs. simulated flow at USGS gaging station 1331250, EFSFSR above Sugar Creek (linear)	5-7
Graph 5-9. Measured vs. simulated flow at USGS gaging station 13311250, EFSFSR above Sugar Creek (logarithmic)	5-7
Graph 5-10. Measured vs. simulated flow at USGS gaging station 13311450, Sugar Creek near Stibnite (linear)	5-8
Graph 5-11. Measured vs. simulated flow at USGS gaging station 13311450, Sugar Creek near Stibnite (logarithmic)	5-8
Graph 5-12. Measured vs. simulated drawdown in wells MWH-A05 and MWH-B05	5-9
Graph 5-13. Measured vs. simulated drawdown in well SRK-GM-21S	5-10

List of Tables

Table 2-1. Summary of Target Groundwater Elevations.....	2-5
Table 3-1. Meteoric Water Balance	3-2
Table 4-1. Simulated Stream Segments	4-3
Table 4-2. Simulated Aquifer Parameters	4-6
Table 5-1. Bulk groundwater-level calibration statistics	5-2



List of Abbreviations

BC	Brown and Caldwell
bgs	below ground surface
DEM	digital elevation model
EFSFSR	East Fork of the South Fork of the Salmon River
ft	foot
HCSM	hydrologic conceptual site model
In/yr	inches per year
JSAI	John Shomaker & Associates, Inc.
Midas Gold	Midas Gold Idaho, Inc.
PRISM	Parameter-Elevation Regressions on Independent Slopes Model
PRO	Plan of Restoration and Operations
Project	Stibnite Gold Project
RMSE	root mean squared error
SFR	Surface Flow Routing
USGS	United States Geological Survey
WRSR	Water Resources Summary Report



Executive Summary

This report presents a numerical model of the hydrologic system of the upper watershed of the East Fork of the South Fork of the Salmon River in north-central Idaho, where Midas Gold Idaho, Inc. (Midas Gold) proposes to develop the Stibnite Gold Project (Project).

The proposed Project would involve excavation of three open pits and building of development rock storage facilities, processing plant, and tailings storage facility. These would involve diversion of groundwater and surface water and consumption and discharge of water, potentially resulting in effects on downstream flow and water quality, and local effects on groundwater levels, stream flows, and water quality in the watershed.

The hydrologic model consists of a long-term meteoric water balance that tracks precipitation, snow accumulation and melt and a numerical groundwater flow model developed using MODFLOW-NWT. The water balance and numerical flow models have been calibrated to groundwater flow and surface water data collected at the site, which represent existing conditions. The model described here is thus referred to as the existing conditions model.

The focus of model calibration has been to simulate seasonal changes in groundwater flow in alluvium/colluvium and overburden, observed groundwater levels, and observed surface flows. The existing conditions model reasonably simulates the annual cycle of snowmelt runoff that provides short-term flow in upland overburden. The model is well calibrated to observed groundwater levels to within approximately 5 feet and accurately represents hydraulic gradients (with a scaled root mean squared error less than 2 percent). The model also reasonably simulates observed stream flows, including spring peak flows and winter base flows.

The calibrated existing conditions model is an appropriate tool to assess changes to the groundwater and surface water flow systems due to mine operations and over the long term after closure. Results from future hydrologic model predictions of the proposed action and alternative(s) will be reported separately and used in other site models and assessments.

Section 1

Introduction

Brown and Caldwell (BC) has prepared this report summarizing work performed to develop a calibrated hydrologic model for the Midas Gold Idaho, Inc. (Midas Gold) Stibnite Gold Project (Project) study area. Model development has proceeded in accordance with the *Final Work Plan: Hydrologic Model of the Upper Watershed of the East Fork of the South Fork of the Salmon River, Stibnite, Idaho* (John Shomaker & Associates, Inc. [JSAI] 2017) (Work Plan). The Work Plan includes details related to available groundwater and surface water data, groundwater and surface water flow conditions, development of the meteoric water balance, and general development of numerical groundwater flow model.

BC has worked in close consultation with JSAI to implement the initial groundwater flow model (developed using the JSAI in-house version of the United States Geological Survey [USGS] groundwater model MODFLOW [McDonald Morrissey Associates 1998]) into MODFLOW-NWT (Niswonger et al. 2011). MODFLOW-NWT includes a Newton-Raphson solution formulation to improve simulation of unconfined groundwater flow and incorporates code changes that preserve mass-balance accounting for dry cells, key for solving problems involving drying and rewetting of model cells, a primary consideration for simulation of seasonal flows in overburden material within the study area.

The hydrologic model described herein is comprised of a long-term meteoric water balance tracking precipitation, snow accumulation and melt, and the numerical groundwater flow model developed using MODFLOW-NWT. The water balance and numerical flow models have been calibrated to groundwater flow and surface water data collected at the site, which represent existing conditions. The model described here is thus referred to as the existing conditions model.

General objectives for the existing conditions model include:

- Develop a meteoric water balance tracking monthly precipitation, snow accumulation, sublimation/evaporation, and melt to estimate runoff and recharge inputs to the surface water and groundwater flow model.
- Develop a numerical model of surface water and groundwater flow in the study area.
- Calibrate the combined water balance and numerical model to closely resemble measured surface water flow rates, groundwater levels, and aquifer test results.

Outputs from the meteoric water balance and calibration of the existing conditions model are discussed in this report.

The calibrated model described here will subsequently be used to estimate the potential impacts of the Project, including:

- Dewatering rates required to develop the open pit mines
- The local effects of dewatering and water management strategies on groundwater levels and stream flows
- Water balances and ranges of surface water and groundwater flows at different locations and for different mine facility footprints, including:

- Post-mining filling rates and water balances for open pits
- Water balances for development rock storage facility footprints
- Water balance for tailings storage facility footprint
- Flow and water balances for stream flow monitoring points

The results from the proposed action model will in turn provide flow inputs to (a) the site-wide water balance model for Project facilities and flows of freshwater, process water, tailings water, and other contact water and (b) water-quality assessments for Project facilities and monitoring points. The model applications and projections listed above will be reported separately.

1.1 Site Background and Project Plan

The study area, shown on Figure 1-1, is the upper watershed of the East Fork of the South Fork of the Salmon River (EFSFSR) in Valley County, Idaho, and includes the Stibnite mining district.

The Stibnite area has been a mining district since the late 19th century. Mining occurred intermittently from the 1890s through the 1990s, with major operations in the 1920s through early 1950s and from the late 1970s through the 1990s.

Existing legacy mining facilities include a tailings impoundment and overlying Spent Ore Disposal Area along Meadow Creek, the Yellow Pine open pit along the EFSFSR, and various adits, tunnels and other underground workings, heap leach pads, rock dumps, and smaller pits throughout the study area. Midas Gold began exploration activities in the area in 2009.

The anticipated life of the Project is approximately 20 years, including approximately 3 years for site cleanup, infrastructure construction, and early restoration activities; 12 to 15 years for mining operations; and 2 to 3 years for final closure and reclamation work. Details of the proposed plan are provided in the Plan of Restoration and Operations (PRO; Midas Gold 2016).

The PRO consists of two primary components: (1) restoration of major legacy impacts from historical mining activities and (2) redevelopment of open-pit mining and reclamation of the three primary ore deposit areas (Yellow Pine pit in the north, West End pit in the northeast, and Hangar Flats pit in the south). Areas of proposed mining activities are shown on Figure 1-2.

1.2 Report Organization

A summary of the general hydrologic conceptual site model (HCSM) is provided in Section 2. Section 3 describes development and results of the meteoric water balance. Section 4 describes the setup of the numerical groundwater flow model, and a description of model calibration is provided in Section 5. Section 6 presents an overall summary of model applications currently under development.

Section 2

Hydrologic Setting and Conceptual Model

Elements of the study area hydrologic and hydrogeologic systems are presented in the Water Resources Summary Report (WRSR; BC 2017) and are also described in the Work Plan. An abbreviated summary is provided here.

The study area is a mountain watershed, with hydrologic conditions dominated by the seasonal patterns of snow accumulation and melt. Snow accumulates throughout the winter and melts in spring and early summer. A part of the melt water is consumed by vegetation in the watershed, while the larger part becomes flow in the EFSFSR.

The spring melt slowly drains to the EFSFSR, attenuated by surface topography and by the permeable layer of soil, colluvium, and alluvium that covers the crystalline bedrock over most of the area, and by evapotranspiration from the heavily vegetated watershed.

Part of the melt water circulates through local groundwater systems in alluvium and weathered bedrock and bedrock fractures that lie along the EFSFSR and its tributaries. The local groundwater systems store spring snowmelt and discharge it to the stream system over the full year. Groundwater flows along and toward the surface channels, eventually entering the stream system.

The local groundwater systems generally function as extensions of the surface water system; they do not extend to great depth and are laterally restricted to the valley bottoms. The valley bottom groundwater flow systems are disconnected from each other by the mountains between them, and are likely compartmentalized along the valley bottoms by bedrock constrictions.

The bedrock of the mountain-block study area consists of igneous and metamorphic crystalline rock units. There are no extensive geologic formations found that would normally form aquifers, such as sedimentary, carbonate, or volcanic rock units. Groundwater flows in shallow weathered bedrock and individual rock fracture networks, but there is no regional groundwater flow system connecting the local groundwater systems.

Key elements of the HCSM supporting elements of the existing conditions model include climate data for the meteoric water balance, surface water flow data, and groundwater system information.

2.1 Climate

The principal climate data used to develop the meteoric water balance are precipitation, temperature, and evapotranspiration. Midas Gold has collected meteorological data in the study area since August 2011, including air temperature, barometric pressure, wind speed, and precipitation. Site data collection is ongoing and will continue through mine operations and post-closure.

Climate data collected at the site is only representative of the last few years and is not sufficient for assessing long-term statistics or trends. The WRSR (BC 2017) includes an analysis of long-term regional climate parameters by the Parameter-Elevation Regressions on Independent Slopes Model (PRISM; www.prism.oregonstate.edu). The PRISM method interpolates a database of climate records

onto a spatial grid covering the United States (Daly et al. 2008). PRISM calculates a climate-elevation regression for each grid location based on data from nearby climate stations where long-term records are available, and on a digital elevation model (DEM). Factors considered in the regression used for interpolation of climate parameters include location, elevation, coastal proximity, topographic facet orientation, vertical atmospheric layer, topographic position, and orographic effectiveness of the terrain.

Analysis of both PRISM model results and the shorter-term site data presented in the WRSR (BC 2017) was used to develop average temperature and evapotranspiration conditions. Average monthly temperatures were estimated to range from 18.8 degrees Fahrenheit in December to 58.1 degrees Fahrenheit in July. Monthly average evapotranspiration rates were estimated to range from 0.7 inches in December and January to 3.3 inches in July, with an average annual total of 21 inches.

Precipitation occurs mostly as winter snowfall, with the main input of water to the surface water and groundwater systems occurring during the spring melt. Precipitation is difficult to measure in the study area because (1) precipitation increases with elevation, (2) the spatial distribution of snow is highly uneven, and (3) processes of sublimation and redistribution of snow by wind occur within the watershed. In addition, snow gaging stations are technically difficult to maintain. Long-term records of precipitation are therefore sparse.

PRISM results include an estimate of monthly precipitation from 1895 through 2016 for the study area. The 122-year series represents the best available estimate of long-term precipitation patterns and includes a range of wet, average, and dry conditions. Annual precipitation from this dataset ranges from about 20 to about 50 inches, with a median of about 30 inches/year (in/yr). An analysis of PRISM data for just the last 30-year normal period of 1981 through 2010 suggested an annual average of approximately 32 in/yr (BC 2017).

The regional-scale PRISM results do not consider stream flow gaging data available for the local study area. The monthly PRISM series was therefore modified for use in the meteoric water balance as described in the Work Plan (JSAI 2017) through comparison to measured discharge rates, resulting in an elevation-weighted, basin average precipitation and an estimate of the study area water balance. That analysis resulted in an estimate of mean annual elevation-weighted precipitation on the watershed reporting to the USGS surface water gage USGS 13311000 of 40 inches, comprised of 19 in/yr average surface flow plus 21 in/yr estimated evapotranspiration.

Use of PRISM-based precipitation, temperature, and evapotranspiration data in the meteoric water balance is discussed in Section 3.

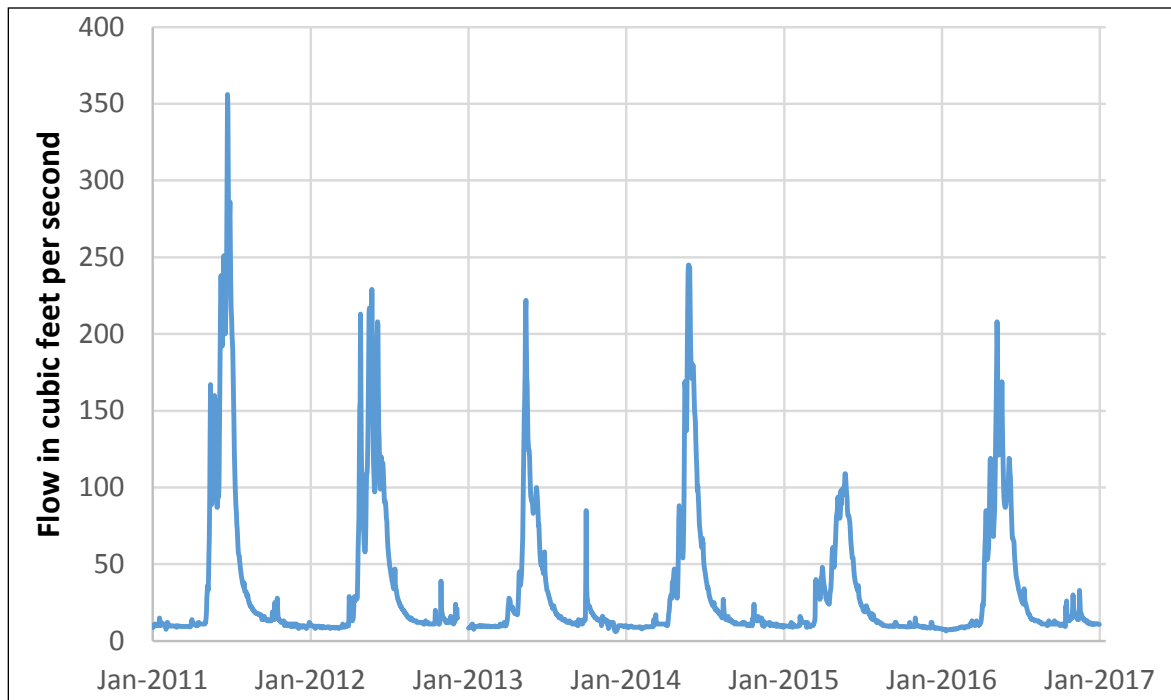
2.2 Surface Water Hydrology

Simulation of surface water flows and interactions between groundwater and surface water is a primary objective of the hydrologic model. The EFSFSR stream network simulated within the model domain is shown on Figure 2-1, including the main EFSFSR channel and tributary streams. The total drainage area in the model domain is about 43 square miles. The full EFSFSR watershed area is about 422 square miles at the confluence with the South Fork Salmon River, with an estimated average annual discharge of about 435,000 acre-feet (HydroGeo, Inc., 2012), equivalent to a basin-average water yield of 19.3 in/yr. Simulation of this stream network in the numerical model is discussed in Section 4.3.2.

Locations of USGS stream flow gages within the study area are shown on Figure 2-2. Historical stream flow data from 2011 through 2016 are generally similar for each USGS gage and indicate that flow is generally characterized by peaks in May and June that are about an order of magnitude higher than base flow in August through February. The magnitude of peak flow is variable, depending

on annual snowfall, but the timing of the annual peak is generally consistent from year to year. The magnitude of base flow is more consistent from year to year than peak flows, indicating consistent groundwater recharge in both wet years and dry years. Graph 2-1 presents an example stream flow hydrograph illustrating the typical seasonality in surface flows in the basin. Additional stream flow hydrographs illustrating this seasonality can be found in the WRSR (BC 2017).

A primary goal of model calibration is to reasonably simulate both peak stream flow events (from runoff estimates from the meteoric water balance model) and stream baseflows from simulated groundwater/surface water interactions.



Graph 2-1. Flow in the EFSFSR at Stibnite (USGS 13311000), linear scale

2.3 Groundwater Hydrogeology

Simulation of groundwater flow is a principal objective for the hydrologic model. Groundwater flow in the study area occurs in the Quaternary unconsolidated deposits in valleys (primarily alluvium, glacial, and glaciofluvial materials, collectively referred to as the alluvial aquifer) and on mountainsides (glacial moraines, colluvial and landslide materials, referred to as overburden). Additional groundwater may also be contributed to the alluvial aquifer from localized permeable weathered zones and fractures in shallow bedrock (SPF 2017). Flow may also occur in permeable geologic structures (fracture zones and faults) within deeper bedrock (SPF 2017).

2.3.1 Groundwater Occurrence and Flow System Boundaries

Alluvial Aquifer. The Quaternary unconsolidated deposits in stream valleys consist of alluvium, glacial materials (e.g., lateral, terminal, and recessional moraines), glaciofluvial deposits (i.e., outwash), and colluvium. These unconsolidated deposits include silt-, sand-, gravel-, and cobble-sized materials. Groundwater flow in these unconsolidated deposits occurs within the pore spaces of the materials and is generally unconfined. Groundwater in the Quaternary unconsolidated deposits enters as recharge from snowmelt, precipitation, and infiltration of surface runoff from upland areas and flow

from underlying fractured bedrock. The groundwater in the unconsolidated deposits discharges primarily to surface streams but may also discharge locally to wetlands, seeps, and springs. The discharge to seeps and springs from unconsolidated deposits sometimes flows only a short distance over the surface before infiltrating back into the unconsolidated materials (SPF 2017).

Hydraulic conductivity estimates for the alluvial aquifer developed hydraulic testing in the study area range from 0.3 to 139 feet (ft)/day, with a mean of 21.2 ft/day (BC 2017). On the slopes above the valley bottoms, there is a variable thickness of soil and colluvium over most of the area. This variably saturated layer also conducts water on a seasonal basis, absorbing snowmelt and gradually draining to the groundwater system and the stream channels.

Bedrock Flow. Groundwater occurrence in bedrock is principally found in and controlled by localized fractures that are generally more shallow than major geologic structures. These localized bedrock fractures are recharged from snowmelt and precipitation on mountainsides and are connected to bedrock fractures beneath alluvial and glacially derived unconsolidated materials in stream valleys. Groundwater flow in bedrock is controlled by topography and the widths and interconnections of fractures. Where these fractures are filled with gouge, alteration products, or other low-permeability materials, groundwater flow may be locally confined (in some cases artesian) or semi-confined—otherwise groundwater in these fractures is unconfined. The groundwater in these fractures discharges to seeps and springs, historical mine workings (e.g., adits) and to streams either directly or through unconsolidated deposits in stream valleys (SPF 2017). Historical mine workings also locally discharge to seeps and springs.

Bedrock hydraulic conductivity estimates from hydraulic testing (BC 2017) range from 3×10^{-4} to 5.9 ft/day (BC 2017). Results of the hydraulic testing of bedrock show a large range of hydraulic conductivities, which is expected when testing both fractured and unfractured portions of the crystalline rock.

In general, no extensive bedrock groundwater flow system has been found. Groundwater is locally contained in fractured bedrock along the valley bottoms and along faults, in isolated compartments or in connection with overlying alluvial systems. The bedrock does not form a distinct regional lower aquifer.

Structure-Controlled Flow. The potential for intermediate-scale groundwater flow in bedrock also exists in larger fault zones, such as the Meadow Creek, West End, and Scout Valley fault zones. Significant groundwater flow in this type of structure requires the major geologic structures to be permeable (e.g., brecciated), physically well-connected, and have hydraulic gradients that would transmit groundwater over significant distances. The Meadow Creek Fault zone and other fault zones in the area include zones of both relatively permeable brecciated materials and relatively impermeable gouge and other low-permeability altered materials. Zones of relatively impermeable materials inhibit regional-scale groundwater flow (SPF 2017). The geologic structures that likely extend to deeper depths in bedrock appear to be connected based on geologic mapping (Stewart et al. 2016); however, the groundwater flow is limited to the planes of these structures and does not extend into the surrounding unfractured bedrock. Where these fault zones cross stream valleys is also where groundwater recharged into the structures at higher elevations would likely discharge to the streambeds. Significant regional-scale groundwater flow is unlikely given the zones of low-permeability materials filling major geologic structures and the likely drainage of these structures where they cross stream valleys that would prevent the development of hydraulic gradients for regional-scale flow.

Hydrogeologic Boundaries. Based on the high topographic relief in the area, groundwater flow is likely predominantly topographically driven with groundwater recharge on mountainsides flowing through shallow fractured bedrock to unconsolidated deposits, discharging mainly in surface water

streams as well as springs and seeps. As such, groundwater flow divides are likely roughly coincident with surface water divides, including the watershed boundary that forms the study area. However, relatively permeable geologic structures in deeper bedrock could—in theory—allow groundwater flow across these surface water catchment areas; or, relatively impermeable geologic structures may compartmentalize flow within these catchment areas. Where these geologic structures cross unconsolidated deposits in stream valleys, groundwater may discharge from the geologic structure to the unconsolidated deposits (i.e., the unconsolidated deposits and streams function as drains for the geologic structures, limiting the potential for groundwater recharged into the geologic structures at higher elevations to flow downgradient across surface watershed boundaries). It should be noted that while discharge from deeper geologic structures into alluvium may occur, no such structures have been identified during extensive recent or historic drilling.

Development of the numerical groundwater flow is focused on simulating alluvial and bedrock groundwater flow as described above. The potential for flow in geologic structures will be assessed through sensitivity analysis during simulation of site operations.

2.3.2 Groundwater Data for Numerical Modeling

Midas Gold has measured groundwater levels at monitoring points in the study area since November 2011. Locations of groundwater elevations used to develop the numerical model are shown on Figure 2-3 and observed well water levels are listed in Table 2-1. The primary groundwater flow system to be simulated in the model is within the valley alluvium and associated glacial and overburden deposits. A groundwater contour map showing alluvial flow conditions is presented in Figure 2-4 (BC 2017). The water levels in Table 2-1 and the contours shown on Figure 2-4 are based on water levels measured in during fall months. Groundwater elevation contours would be expected to generally apply to all seasons and time periods, as the seasonal variability of groundwater levels, at less than +/- 10 ft (BC 2017), is small compared to the relief in the study area.

An assessment of the thickness of the soil, colluvial, and alluvial overburden has been prepared by Midas Gold based on geologic logging and surface geophysical data. The assessment was designed to determine near-surface permeable zones, and the results are presented on Figure 2-5. The greatest thicknesses of alluvium lie along the valley bottoms, with a contiguous large thickness in Meadow Creek Valley that forms a significant alluvial aquifer. Note that this assessment is focused on areas of proposed mining activities and does not cover the entire extent simulated in the hydrologic model.

Table 2-1. Summary of Target Groundwater Elevations

Well Name	X-Coordinate ¹	Y-Coordinate ¹	Observed Groundwater Elevations (ft amsl)
MWH-A13	2,734,047	1,183,853	6,362
Gestrin_Airstrip	2,732,369	1,178,102	6,527
MWH-A02_(SRK-GM-25S)	2,729,630	1,175,698	6,595
MWH-A03	2,731,663	1,173,950	6,917
MWH-A04	2,731,116	1,177,484	6,547
MWH-A05	2,732,316	1,178,247	6,527
MWH-A07	2,733,678	1,179,556	6,490
MWH-A08	2,734,676	1,179,733	6,511
MWH-A09	2,733,926	1,180,989	6,456
MWH-A10	2,734,017	1,181,899	6,425

Table 2-1. Summary of Target Groundwater Elevations

Well Name	X-Coordinate ¹	Y-Coordinate ¹	Observed Groundwater Elevations (ft amsl)
MWH-A12	2,734,471	1,182,808	6,448
MWH-A14	2,733,314	1,187,130	6,236
MWH-A15	2,732,700	1,186,106	6,302
MWH-A17_(SRK-GM-05S)	2,731,247	1,189,949	6,111
MWH-A18	2,731,860	1,191,425	5,956
MWH-A19_(SRK-GM-08S)	2,731,383	1,191,508	5,967
MWH-B02	2,728,214	1,176,114	6,620
MWH-B13	2,734,049	1,183,844	6,359
SRK-GM-02S	2,730,431	1,191,801	5,979
SRK-GM-03S	2,730,787	1,191,561	5,981
SRK-GM-04S	2,731,271	1,190,827	6,046
SRK-GM-07S	2,733,145	1,186,295	6,280
SRK-GM-09S	2,731,595	1,191,126	5,983
SRK-GM-10S	2,731,898	1,190,443	6,007
SRK-GM-11S	2,732,238	1,187,616	6,161
SRK-GM-12S	2,732,440	1,187,280	6,181
SRK-GM-21S	2,732,335	1,178,270	6,522
SRK-GM-22S	2,731,743	1,177,643	6,541
SRK-GM-23S	2,730,989	1,177,159	6,547
SRK-GM-24S	2,729,708	1,176,384	6,585
SRK-GM-26S	2,728,817	1,175,184	6,599
SRK-GM-27S	2,727,669	1,174,889	6,604
SRK-GM-28S	2,727,102	1,175,524	6,611
SRK-GM-29S	2,727,233	1,175,196	6,606
SRK-GM-30S	2,727,151	1,174,770	6,606
SRK-GM-31S	2,726,772	1,175,410	6,614
SRK-GM-34S	2,723,029	1,174,469	6,926
SRK-GM-35S	2,726,669	1,175,127	6,612
SRK-GM-37S	2,726,707	1,174,641	6,615
SRK-GM-38S	2,726,310	1,175,324	6,617
SRK-GM-40S	2,726,275	1,174,762	6,618
SRK-GM-41S	2,726,037	1,175,011	6,618
SRK-GM-42S	2,734,500	1,180,860	6,502
SRK-GM-43S	2,734,658	1,180,664	6,511
MWH-A01	2,723,520	1,173,983	6,788
MWH-B03	2,731,655	1,173,946	6,920

Table 2-1. Summary of Target Groundwater Elevations

Well Name	X-Coordinate ¹	Y-Coordinate ¹	Observed Groundwater Elevations (ft amsl)
MWH-B04	2,731,126	1,177,484	6,545
MWH-B05	2,732,323	1,178,269	6,525
MWH-B07	2,733,678	1,179,568	6,491
MWH-B09	2,733,927	1,180,999	6,444

¹Coordinates in Idaho State Plane West, North American Datum of 1983, U.S. Feet.



Section 3

Meteoric Water Balance

The hydrologic model was developed by combining a spreadsheet-based meteoric water balance with a numerical groundwater and surface-water flow model developed using MODFLOW-NWT (Niswonger et al. 2011).

The model computational structure is shown on Figure 3-1. Monthly snowmelt and rainfall computed by the meteoric water balance are input to the numerical model as groundwater recharge and surface water runoff. The numerical model then computes monthly groundwater levels and surface water flows throughout the model domain, as well as surface water flow exiting the domain. Results of the meteoric water balance are described below.

Inflows to the model from snowmelt and rainfall are computed using a spreadsheet-based monthly water balance that tracks precipitation as rain and/or snow, subject to sublimation, snowpack accumulation, snowmelt, and evaporation. The meteoric water balance is described by equation (Equation 3-1):

$$M_k = P_k + (S_{k-1} - S_k) - E_k \quad (3-1)$$

Where:

P_k = precipitation, month k

S_k = snowpack; $(S_{k-1} - S_k)$ is snowmelt for month k

E_k = sublimation + evapotranspiration

M_k = snowmelt + rainfall

The meteoric water balance sequence is as follows:

- Monthly precipitation from the PRISM dataset is entered for the period 1895 through 2016 and then scaled up by a factor of 1.215 based on stream flow and potential evaporation data as described in the Work Plan (JSAI 2017). This results in a long-term average annual precipitation on the order of 40 in/yr.
- Precipitation falling in November through March is assumed to be snow. Precipitation falling in May through August is assumed to be rainfall, while precipitation falling in the other months is portioned as half snow and half rainfall.
- Snowpack is accrued monthly and is subject to sublimation and melt.
 - Sublimation is subtracted from the snowpack. The maximum sublimation rate is initially assumed at 0.04 inches per day (1 millimeter/day [Jones 2006]). The actual monthly sublimation is computed as the maximum rate, limited to the available snowpack.
 - The fraction of snowpack that melts is estimated as a function of monthly average temperature from the PRISM dataset. The melt fraction is estimated as a function of temperature using the degree-day equation, as described in the Work Plan:

$$\min(1, \max(0, [t - t_f] / [t_m - t_f])) \quad (3.2)$$

Where:

t_m = “melting temperature,” the threshold temperature for complete melting

t_f = “freezing temperature,” the threshold temperature for melt to stop

So, for $t > t_m$, all available snowmelts. For $t < t_f$, no melt occurs. For t between t_m and t_f , a fraction of the snowmelts in proportion to t . The melting and freezing temperatures were adjusted to match the observed timing of annual high flows.

- Any rain falling in the month is added to snowmelt total available water. Evapotranspiration is then subtracted from the available water. Evapotranspiration was estimated as a linear function of available snowmelt and rainfall and on potential evaporation as a function of elevation. The computation of evapotranspiration is as follows:

$$\text{evaporation} = \min(Q, \min(1, aQ+b)*PET)$$

Where:

Q = snowmelt + rainfall

PET = potential evapotranspiration, computed from temperature, elevation, and latitude

a and b = empirical coefficients

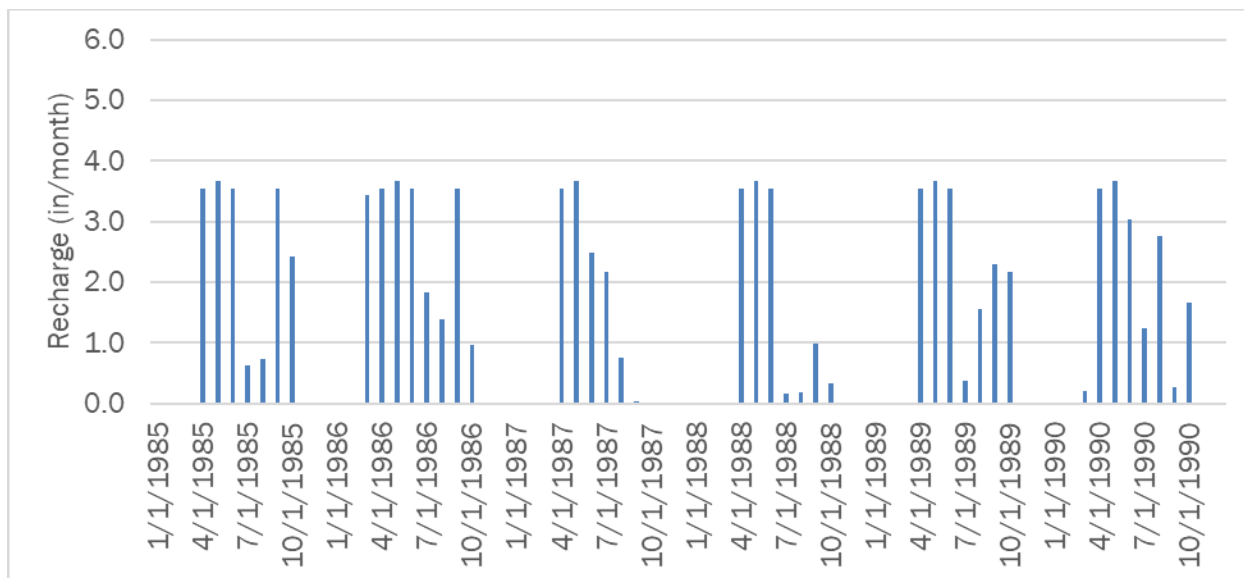
The parameters of the water balance model are adjusted to match measured stream flows over the period 2011 through 2016.

- The amount of water after evapotranspiration is subtracted is available to recharge groundwater or produce runoff at the surface. Water is assigned to recharge first, up to a maximum value (assumed to be 0.01 ft/day based on calibration adjustments). Available water above the maximum recharge is accounted as surface runoff.

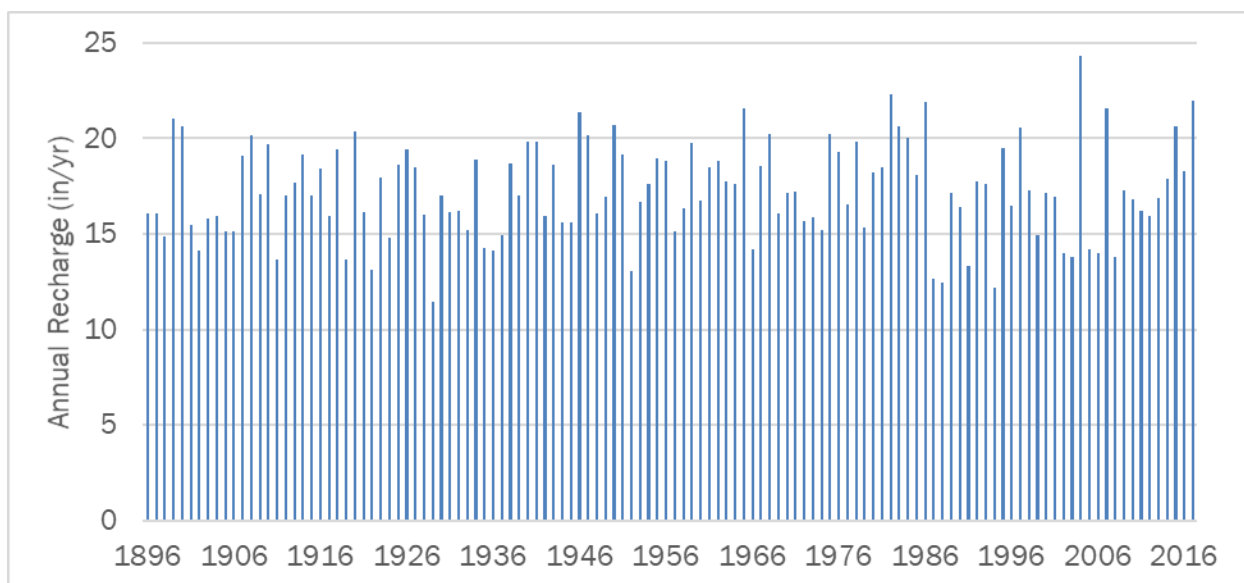
Preliminary meteoric water balance parameters are summarized on Table 3-1.

Table 3-1. Meteoric Water Balance		
Parameter	Value	Unit
Melting temperature t_m	12	degree Celsius
Freezing temperature t_f	-2.5	degree Celsius
Evapotranspiration coefficient a	0.0025	inch ⁻¹
Evapotranspiration coefficient b	0.0276	unitless

Monthly recharge and surface runoff values were developed for the entire 122-year PRISM data period. Graph 3-1 shows a period of monthly recharge estimates representing 1985 through 1990, shown as an example of short-term recharge variation. Monthly recharge varies between zero in fall and winter months up to a maximum of 3.7 in/month during spring snowmelt. Annual total recharge is shown on Graph 3-2. Annual recharge for the 122-year period varies between a low of 11.5 inches in 1929 to a high of 24.3 inches in 2004. Annual average recharge is estimated from the meteoric water balance at 17.2 in/yr.

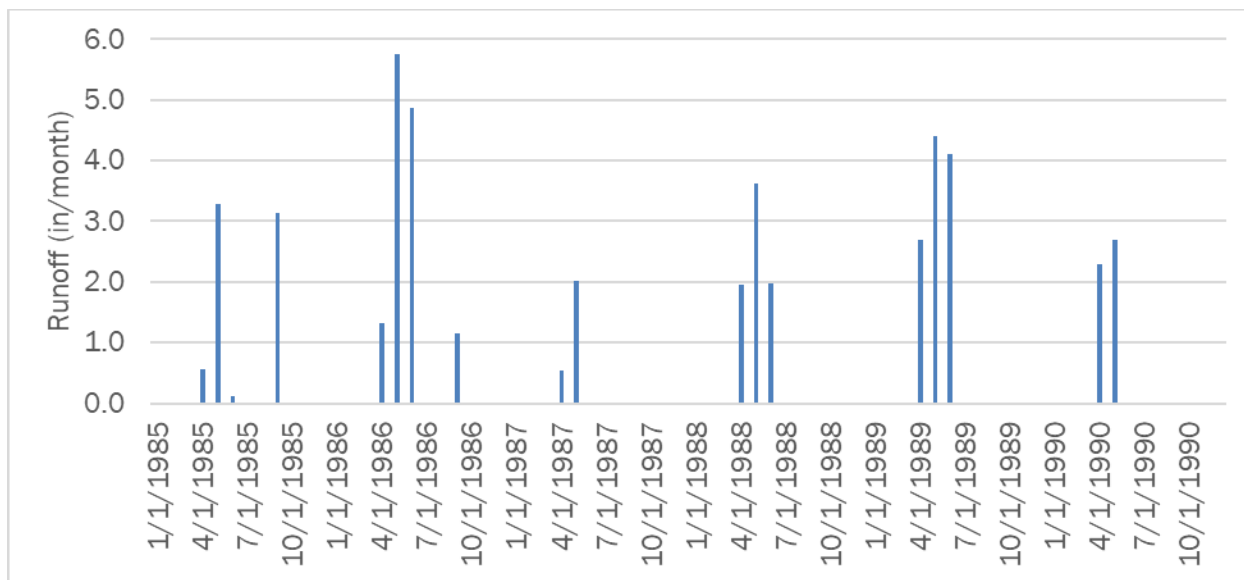


Graph 3-1. Example of short-term monthly recharge estimates 1985–1990

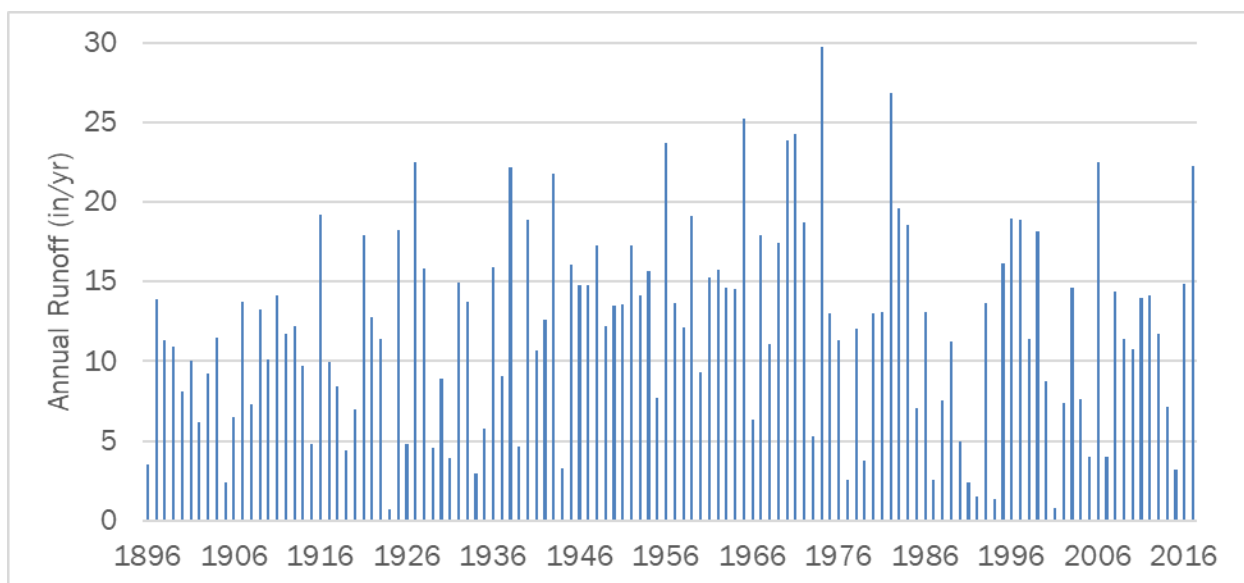


Graph 3-2. Annual recharge estimates

Graph 3-3 shows a period of monthly runoff estimates representing 1985 through 1990, shown as an example of short-term runoff variation. Monthly runoff varies between zero in fall and winter months to a maximum of 15.5 inches. Annual totals of runoff are shown on Graph 3-4. Annual runoff for the 122-year period varies from a low of 0.71 inches in 1924 to a high of 29.7 inches in 1974. Average annual surface runoff is estimated at 12.0 in/yr.



Graph 3-3. Example of short-term monthly runoff estimates 1985–1990



Graph 3-4. Annual runoff estimates

Section 4

Numerical Model Setup

The numerical model was developed using the USGS MODFLOW-NWT model (Niswonger et al. 2011). MODFLOW-NWT was chosen because it includes a Newton-Raphson solution formulation to improve simulation of unconfined groundwater flow, intended for solving problems involving drying and rewetting of model cells. A component of the HCSM includes seasonal flows in overburden occurring in upland areas during spring snowmelt, with a pattern of wetting during the spring followed by drying in the fall and winter. While these flows are a small part of the overall groundwater system, use of MODFLOW-NWT allows for a reasonable simulation of this seasonality in the system.

This section discusses setup of the groundwater flow model, including the simulation period, lateral and vertical model discretization, model boundary conditions, and model parameterization.

4.1 Simulation Period

Model simulations initially followed monthly time steps for the 122-year (1895 through 2016) historical period including the 2011 through 2016 calibration period. Model testing showed that a pattern of seasonal fluctuations stabilizes within the first 3 to 5 years of the simulation period. Once general calibration was achieved, the model simulation period was focused to simulate conditions between 1985 and 2016, using initial heads developed from the full 122-year model. The 1985 through 2016 model was used for finetuning model calibration.

A standard steady-state solution was not developed because the system is constantly in a seasonal flux and has no steady state. The system is constantly either filling up (wetting) or draining down (drying). Recharge to and discharge from the groundwater system are not steady or constant but are continually changing over the seasonal cycle. Instead, a seasonal steady-state solution was developed by running the long-term transient simulation iteratively. Final conditions (ending groundwater levels) from one simulation were used as the starting water levels for the next, until the net cumulative flow from storage was near zero.

Inputs to the model include (1) discretization of the model domain, (2) hydraulic parameters that control the flow of water within the model domain, and (3) boundary conditions that control the addition and removal of water to and from the model domain. These inputs are presented below.

4.2 Model Discretization

The model grid consists of 224 rows, 145 columns, and 3 vertical layers. The lateral model domain is shown on Figure 4-1, with the model grid shown on Figure 4-2. Horizontal grid spacing ranges from 30 ft in the vicinity of the Hangar Flats pit out to approximately 330 ft within the rest of the model domain. Finer grid spacing was used in the Hangar Flats area to facilitate more refined assessments of open pit dewatering.

The model is structured with three layers, as follows:

- Layer 1 represents the alluvial aquifer and overburden. The flow within the layer is unconfined. The bottom elevation of the overburden (Layer 1) was computed using land surface elevations and the overburden thickness shown on Figure 2-5. High resolution LiDAR land surface elevation data were used for the proposed mining areas. Outside of these

areas, surface elevations from a USGS National Elevation Dataset 1-arc-second (approximately 30 meters) DEM were used. Figure 4-3 shows the extent of analysis of the overburden thickness in relation to the entire model domain. Areas outside of the mapped thickness are considered to have limited near surface flow contributions since these locations are generally at higher elevations and outside of the primary alluvial flow zones. Therefore, the overburden thickness outside of the mapped thickness area was assumed 15 ft.

In the main valley bottoms, the overburden forms an aquifer that is recharged seasonally during spring snowmelt and discharges water to the stream system during spring, summer, and early fall periods. Above the valley bottoms the overburden does not form an aquifer, but it retains melt water in storage that slowly drains downward into the bedrock or downhill to the groundwater and surface water system below. A key component of flow in Layer 1 is cell rewetting, used to allow model cells representing overburden to seasonally rewet during the annual melt and then become dry later in the season. This requires correct mass-balance accounting for dry cells, a feature not implemented in USGS MODFLOW codes prior to the release of MODFLOW-NWT.

- Layer 2 represents near-surface bedrock. The shallow upper bedrock is considered to be more weathered and fractured and permeable along the main surface drainages and underneath overburden material on hillslopes. Some groundwater flow and storage likely occurs in the upper part of the bedrock, as fracturing decreases with depth. Layer 2 is simulated as a variably saturated layer in MODFLOW-NWT, and flow varies seasonally between confined and unconfined.
- Layer 3 represents nearly impermeable bedrock at depth. Groundwater flow in Layer 3 is limited by low hydraulic conductivities and is confined. The total thickness simulated by Layers 2 and 3 is 1,000 ft. This was designed to allow for simulation of groundwater flow into the Hangar Flats pit from both permeable and nearly impermeable bedrock zones.

Figures 4-4 and 4-5 present cross sections through the model domain illustrating vertical layering.

4.3 Model Boundary Conditions

For the existing conditions model described here, water enters the model domain primarily through surface recharge, with minor flows from stream losses. Water discharges from the model domain as flow to surface streams. Anthropogenic boundary conditions including pumping from wells and open-pit dewatering will be added to model at a later date to simulate the proposed mining activities.

Water consumed by evapotranspiration is accounted for in the meteoric water balance described above and is not directly simulated in the numerical model. Although evapotranspiration of groundwater occurs from the low-lying areas where groundwater is present, the same areas also receive substantial recharge from snowmelt and runoff and discharge water to the stream system. The accounting of evapotranspiration within the meteoric water balance is thus considered an appropriate simplification.

4.3.1 Recharge

Monthly recharge rates from the meteoric water balance are added to the model using the MODFLOW Recharge Package. Recharge was initially added to the model as a single value covering the entire model domain. Model testing performed during calibration indicated that areas within Layer 1 assigned a thickness of 15 ft (as described in Section 4.2) were consistently flooded when the full amount of recharge was added to this relatively thin flow zone and thus likely have a lower

maximum recharge rate than estimated in the meteoric water balance at the basin scale. Simulations resulted in improved calibrations when less recharge was added to these areas. The calibrated existing conditions model uses 1/3 of the total recharge in areas where Layer 1 is 15 ft thick or less, as shown on Figure 4-6. Water not recharged in these areas was rerouted as surface runoff to adjacent streams, as described in the following section.

4.3.2 Stream Flow

Flows in surface streams and creeks were simulated using the MODFLOW Surface Flow Routing (SFR) package. Stream cells are grouped into segments to define the stream network; each segment defines a length of stream, with a specified downstream segment. Simulated segment reaches are shown on Figure 4-7 and listed in Table 4-1.

Surface runoff computed in the meteoric water balance is added to the numerical groundwater model at the upstream end of each segment based on the watershed area feeding that segment (Table 4-1). For each cell within a segment, infiltration to groundwater or discharge from groundwater is computed, limiting infiltration to available stream flow. The computed infiltration or discharge is added or subtracted to the simulated stream flow, and the resulting total flow, if any, is passed to the next cell downstream. Accumulated surface flow is then output at the locations of the USGS gages where data are available for comparison during calibration.

Stream cell parameters include stream bed elevation, stream stage elevation (height of water above the stream bed), and stream bed conductance (a measure of permeability of materials between the streambed and aquifer). Flow between stream cells and the corresponding aquifer model cell is computed based on stream cell conductance and the hydraulic gradient between the stream stage and the aquifer head. When aquifer heads are higher than the stream stage, flow from the aquifer to the stream is predicted. When aquifer heads are lower than the stream stage, flow from the stream to the aquifer is predicted. Losses from the stream to the aquifer are further limited by the amount of simulated flow available in the stream.

Stream bed elevations were developed by overlaying the model stream cells on site topography data and using the minimum topographic elevation occurring within area of the model cell. Stream stage elevations were assumed to be 2 ft higher than the stream bed elevation (i.e., 2 ft depth of water is assumed for all streams) and were fixed for all stream cells throughout the model simulations. Stream bed conductance is a single lumped parameter that is a function of stream length and width, stream bed thickness, and streambed hydraulic conductivity. Initial conductance estimates were based on assumed values of the above parameters. Conductance values were then modified during calibration. Final stream conductance values ranged from a low of approximately 217 to a high of 29,000 ft⁻¹, depending upon cell size hosting the stream cell.

Table 4-1. Simulated Stream Segments

Segment Number	Reach Name	Catchment Area (km ²)	Downstream Segment Number
1, 2, 3, 4, 5	Meadow Creek 1	8.88	9
6, 7, 8	Meadow Creek Trib 1	4.71	9
9, 10, 11	Meadow Creek 2	4.09	15
12, 13, 14	Blowout Creek	6.35	15
15	Meadow Creek 3	1.97	43
16	EFSFSR 1	3.78	18
17	EFSFSR Trib 1	1.4	18

Table 4-1. Simulated Stream Segments

Segment Number	Reach Name	Catchment Area (km²)	Downstream Segment Number
18, 19, 20, 21, 22	EFSFSR 2	0.83	28
23, 24, 25, 26, 27	Fern Creek	4.38	28
28	EFSFSR 3	0.52	34
29, 30, 31, 32, 33	EFSFSR trib 2	6.22	34
34	EFSFSR 4	0.88	36
35	EFSFSR trib 3	0.49	36
36, 37, 38	EFSFSR 5	0.96	38
39	Rabbit Creek	1.66	40
40, 41, 42	EFSFSR 6	2.56	40
43	EFSFSR 7	1.17	45
44	Garnet Creek	1.06	45
45	EFSFSR 8	2.02	55
46, 47, 48, 49, 50, 51, 52, 53, 54	Fiddle Creek	5.28	55
55	EFSFSR 9	0.44	57
56	Midnight Creek	2.07	57
57, 58	EFSFSR 10	1.11	99
59	Hennessy Creek	1.89	99
60, 61, 62, 63, 64	Cane Creek 1	4.71	66
65	Cane Creek trib 1	2.33	66
66	Cane Creek 2	0.41	70
67, 68, 69	Cane Creek trib 2	2.18	70
70	Cane Creek 3	1.19	72
71	Cane Creek trib 3	0.61	72
72	Cane Creek 4	0.05	80
73	Sugar Creek 1	4.12	77
74	Pyramid Creek trib 1	1.5	76
75	Pyramid Creek 1	3.7	76
76	Pyramid Creek 2	0.31	77
77	Sugar Creek 2	1.92	79
78	Sugar Creek Trib 1	3.44	79
79	Sugar Creek Trib 2	2.26	80
80	Sugar Creek 3	2.43	88
81, 82, 83, 84, 85, 86, 87	Cinnabar Creek	8.03	88
88	Sugar Creek 4	0.05	90
89	Sugar Creek Trib 3	0.8	90
90, 91, 92	Sugar Creek 5	3.08	94

Table 4-1. Simulated Stream Segments

Segment Number	Reach Name	Catchment Area (km ²)	Downstream Segment Number
93	Sugar Creek Trib 4	0.7	94
94	Sugar Creek 6	0.05	96
95	Sugar Creek Trib 5	1.61	96
96	Sugar Creek 7	1.79	98
97	West End Creek	1.58	98
98	Sugar Creek 8	1.35	99
99	EFSFSR 11	0.16	N/A

4.4 Aquifer Physical Parameters

Hydraulic conductivity estimates for the model were developed to represent general, regional-scale aquifer conditions. Figures 4-8 and 4-9 show hydraulic conductivity zonations for model Layers 1 and 2. Layer 1 includes separate zones for alluvium/colluvium in valleys and along stream course and overburden material in upland areas that is subject to drying and rewetting in the annual cycle. Layer 2 includes zones for more permeable weathered and fractured rock in valleys and along stream courses, more permeable bedrock in the Hangar Flats area (suggested by available data), and less permeable rock in upland areas subject to seasonal variations in overlying overburden saturation. Bedrock in Layer 3 is simulated using a single low hydraulic conductivity estimate. Finer, local-scale zonations were not included in the model, as reasonable calibrations were achieved using regional-scale parameter estimates.

The presence of silts and clays in the alluvium contribute to potential restriction in vertical groundwater flow. Variations in vertical hydraulic conductivities were tested during model calibration, and ratios of 10:1 and 100:1 (lateral to vertical hydraulic conductivity) were used in Layer 1 in the model.

For flow in unconfined model layers (model Layer 1, and seasonally, Layer 2), MODFLOW-NWT uses a “total” storage approach, adding confined (specific) storage to the specific yield. For confined flow, the model uses specific storage. Constant values of specific yield (0.125) and specific storage ($1 \times 10^6 \text{ ft}^{-1}$) were used for Layer 1. In Layer 2, less fractured bedrock in upland areas was assigned a specific yield of 0.01, while more weathered and fractured bedrock underneath valleys and stream courses was assigned a higher specific yield of 0.025 (Figure 4-10). Specific storage for all bedrock (Layers 2 and 3) was $1 \times 10^6 \text{ ft}^{-1}$.

Final aquifer parameters developed through calibration are summarized in Table 4-2.

Table 4-2. Simulated Aquifer Parameters				
Hydrogeologic Unit	Hydraulic Conductivity (ft/day)	Vertical Anisotropy Ratio	Specific Yield	Storage Coefficient (ft⁻¹)
Layer 1				
Valley alluvium/colluvium	20.0	100:1	0.125	1 x 10 ⁶
Upland overburden	8.0	10:1	0.125	1 x 10 ⁶
Layer 2				
Non-fractured rock	0.0075	1:1	0.01	1 x 10 ⁶
Moderately fractured rock	0.5	1:1	0.025	1 x 10 ⁶

Section 5

Model Calibration

Model calibration focused on three primary areas:

- Reasonable simulation of seasonal wetting and drying of upland overburden during annual snowmelt periods
- Simulation of observed groundwater elevations
- Simulation of observed stream flow conditions, focusing on late-season baseflow conditions

In addition, simulations of the 30-day Gestrin Airstrip well aquifer test were performed.

Model parameters, including meteoric water balance parameters, aquifer physical parameters, streambed conductances, and application of recharge were adjusted to obtain agreement with observed conditions. The final calibration represents a balance between the calibration objectives, as certain parameter modifications may have improved the model's ability to simulate one condition (such as improved simulation of groundwater elevations) while degrading the model's match in other areas (such as degraded matches to observed surface flows). The final set of model parameters achieves a good balance between all model calibration objectives.

The following sections discuss simulation of seasonal groundwater fluctuations, calibration to observed groundwater levels, calibration to surface water flows, and simulation of the Gestrin well test.

5.1 Seasonal Groundwater Fluctuations

One goal for the existing conditions model was to provide a reasonable simulation of the seasonal cycle of snowmelt providing recharge to upland overburden, with associated groundwater flows through the overburden to the valley alluvium. The existing conditions model simulates annual drying and rewetting of overburden, with saturated flow in the upland overburden generally occurring in March or April through September or October.

Figure 5-1 shows the simulated water table (including both saturated overburden and areas where first groundwater is in bedrock). The simulated water table closely follows topography, as expected. The extent of saturated alluvium/overburden in Layer 1 representing late winter conditions (February 2015) is shown on Figure 5-2. Late-winter groundwater flow is limited to valleys and stream courses in the study area. Figure 5-3 presents the extent of saturated alluvium/overburden in mid-summer (July 2015). As shown on the figure, large areas of Layer 1 have re-saturated and groundwater flow occurs within a wide area of upland overburden in mid-summer. This simulated pattern repeats seasonally, with variations based on the magnitude of monthly recharge to the system.

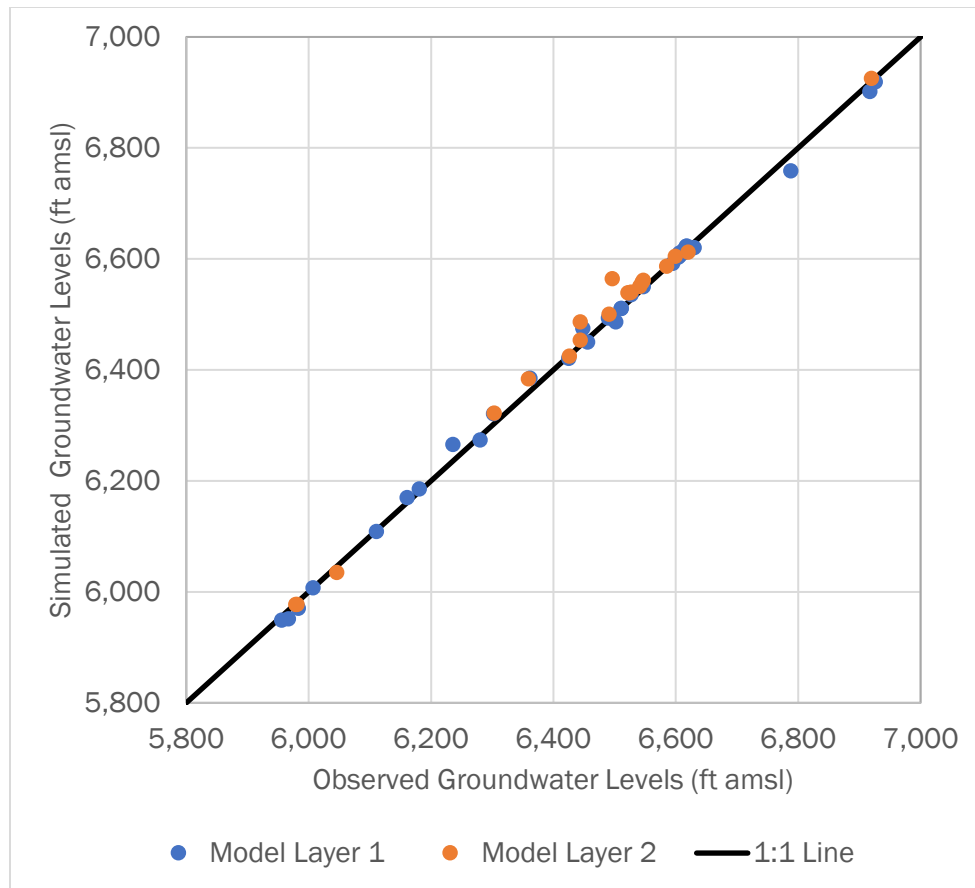
5.2 Groundwater Levels

The existing conditions model was generally calibrated to observed groundwater levels. Analysis of how well the model simulates observed conditions is based on statistics related to model residuals (the difference between simulated and observed groundwater levels). Standard calibration statistics include the average residual, absolute average residual, root mean squared error (RMSE, which gives greater weight to larger residuals), and the scaled RMSE (RMSE divided by the total change in

measured head, a measure of how well the model simulates groundwater flow gradients). Table 5-1 provides a summary of these statistics for the model. It is important to note that an industry defined statistical range that identifies a well calibrated model does not exist, since modeling by necessity requires subjectivity and the acceptability of a calibration is directly dependent on the modeling objective (Anderson et al. 2015).

Table 5-1. Bulk groundwater-level calibration statistics	
Statistic	Value
Residual mean (ft)	-4.60
Absolute residual mean (ft)	10.54
Sum of squared errors (ft)	1.39E+04
Root mean squared (RMS) error (ft)	8.28
Minimum residual (ft)	-68.7
Maximum residual (ft)	29.2
Number of observations*	55
Range in observations (ft)	970
Scaled RMS error (%)	1.6

Given the overall objectives of the Existing Conditions Model, the model is considered well calibrated to observed water levels and the general hydraulic gradients. Groundwater levels are simulated to within approximately 5 ft on average, with simulated levels being slightly higher than those observed. The scaled RMSE is 2 percent, representing good calibration to the regional hydraulic gradient. Graph 5-1 presents a scatterplot comparing simulated and observed values. The majority of the groundwater level targets fall near the 1:1 line, indicative of good calibration.

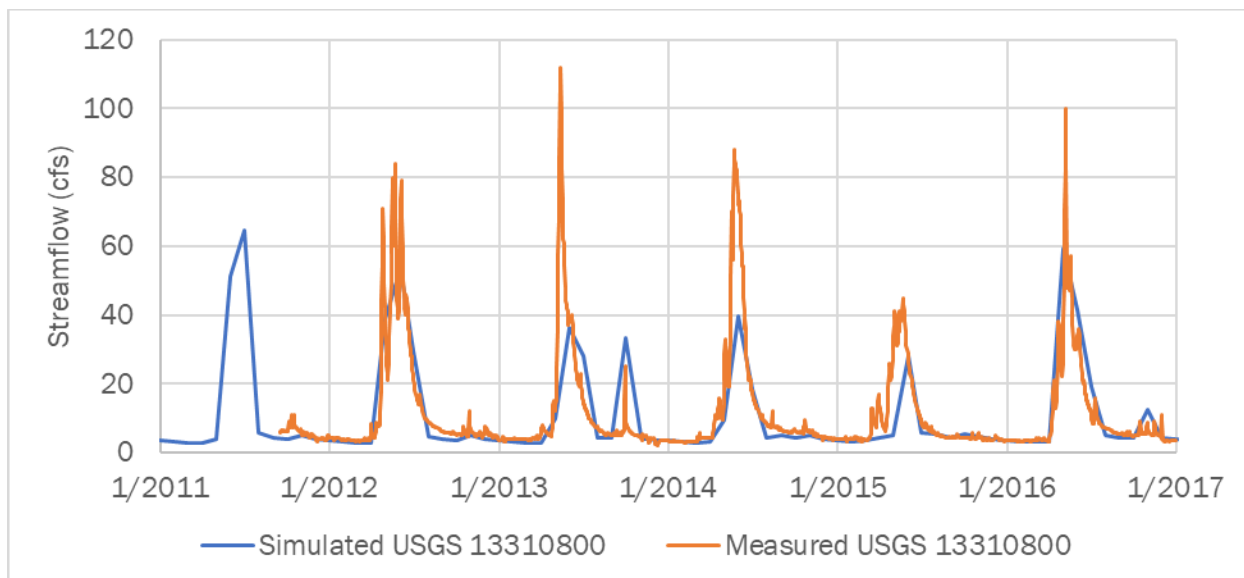


Graph 5-1. Scatterplot showing simulated versus observed water levels

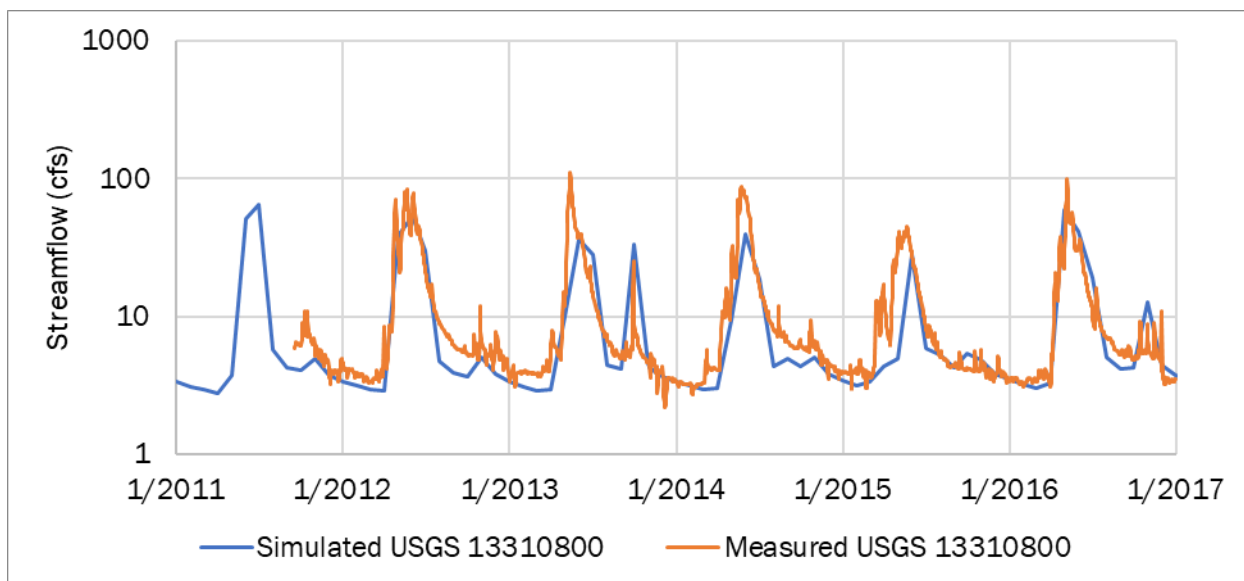
5.3 Surface Water Flows

Simulated surface flows were compared to measured flows at USGS gage locations within the study area that have available flow data between 2011 and 2016. Gage locations are shown on Figure 2-2. Measured and simulated flows are compared on both logarithmic (highlighting low flows) and linear (highlighting high flows) scales in Graphs 5-2 through 5-11. Note that simulated flow rates represent monthly values while the observed data is daily, such that the model is not expected to simulate exact daily peaks.

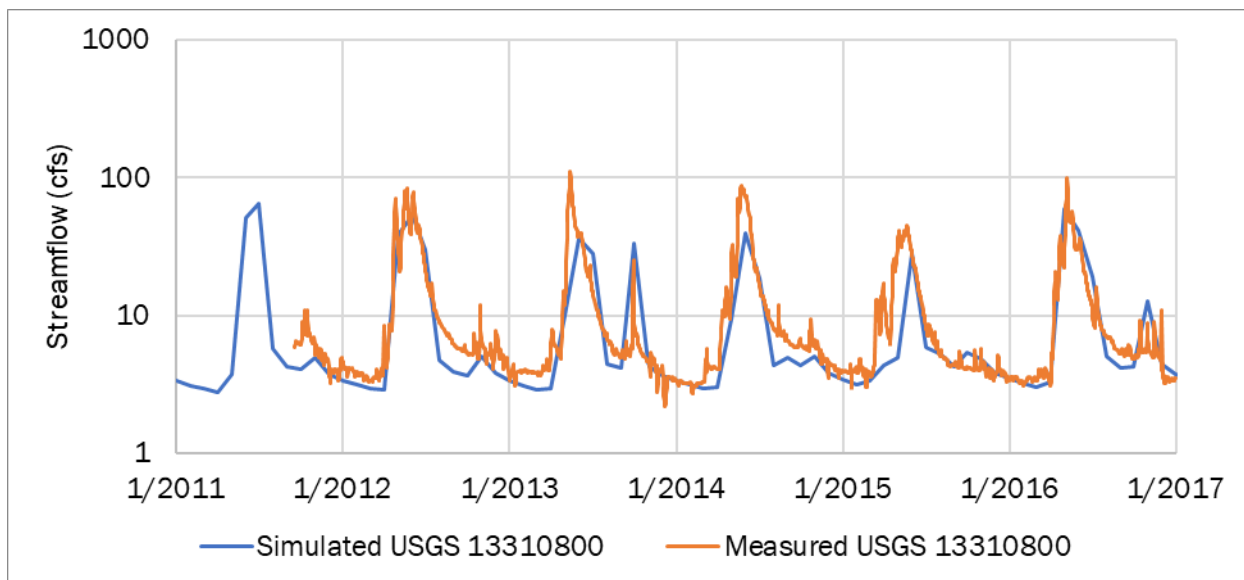
The model reproduces the approximate timing and the approximate magnitude of the annual runoff hydrograph, as well as winter low flows (baseflow), which indicate the magnitude of groundwater discharge. The model is considered well calibrated to observed surface flows.



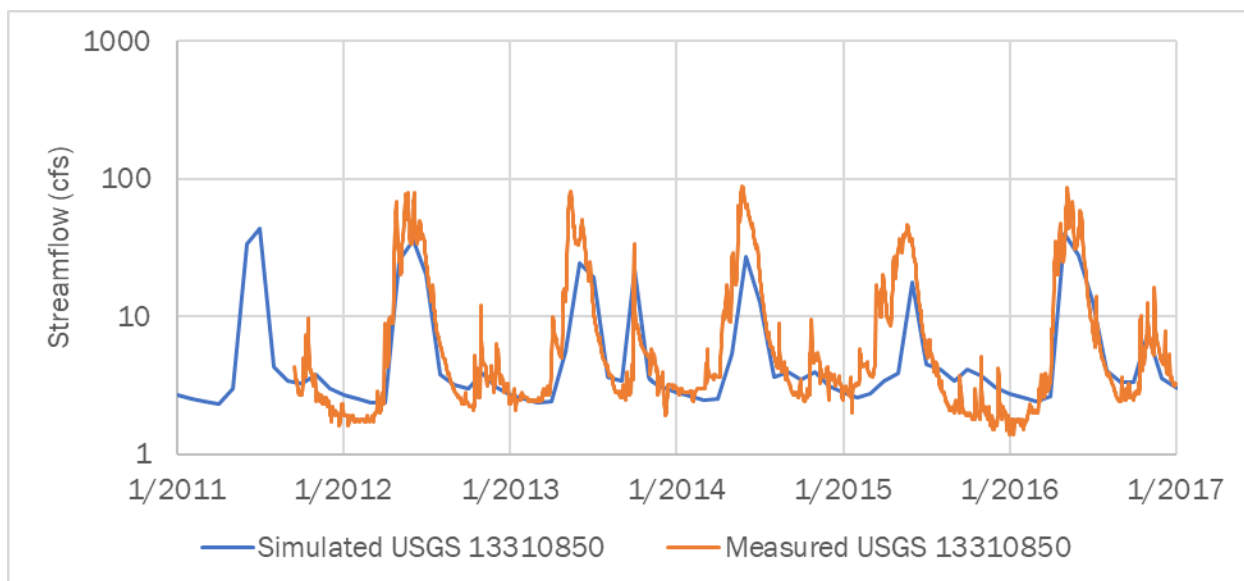
Graph 5-2. Measured vs. simulated flow at USGS gaging station 13310800, EFSFSR above Meadow Creek (linear)



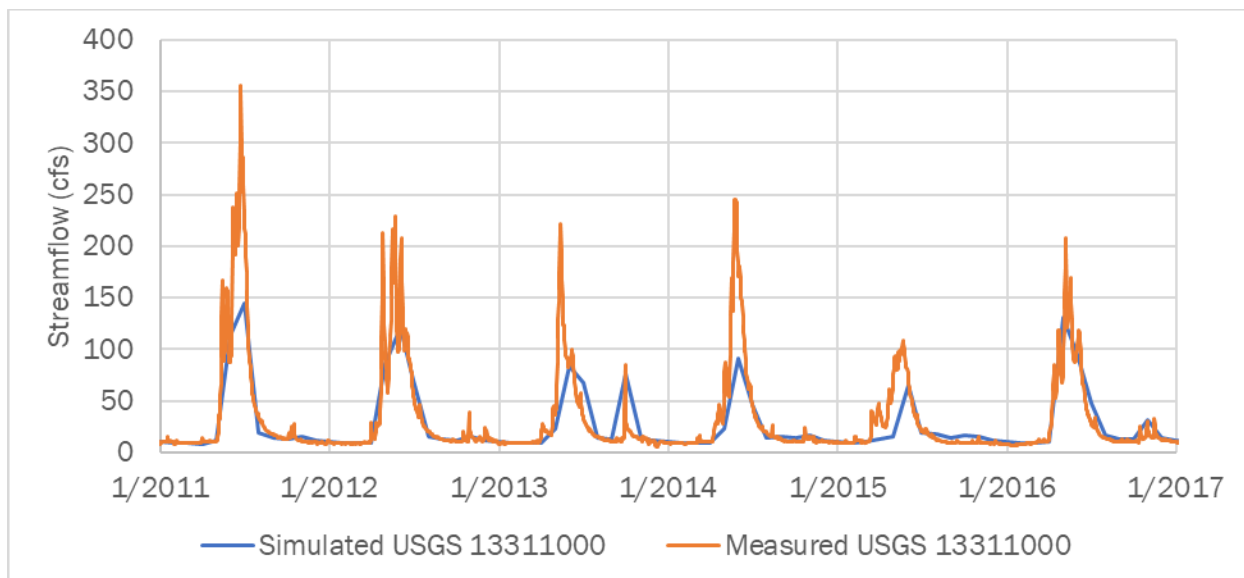
Graph 5-3. Measured vs. simulated flow at USGS gaging station 13310800, EFSFSR above Meadow Creek (logarithmic)



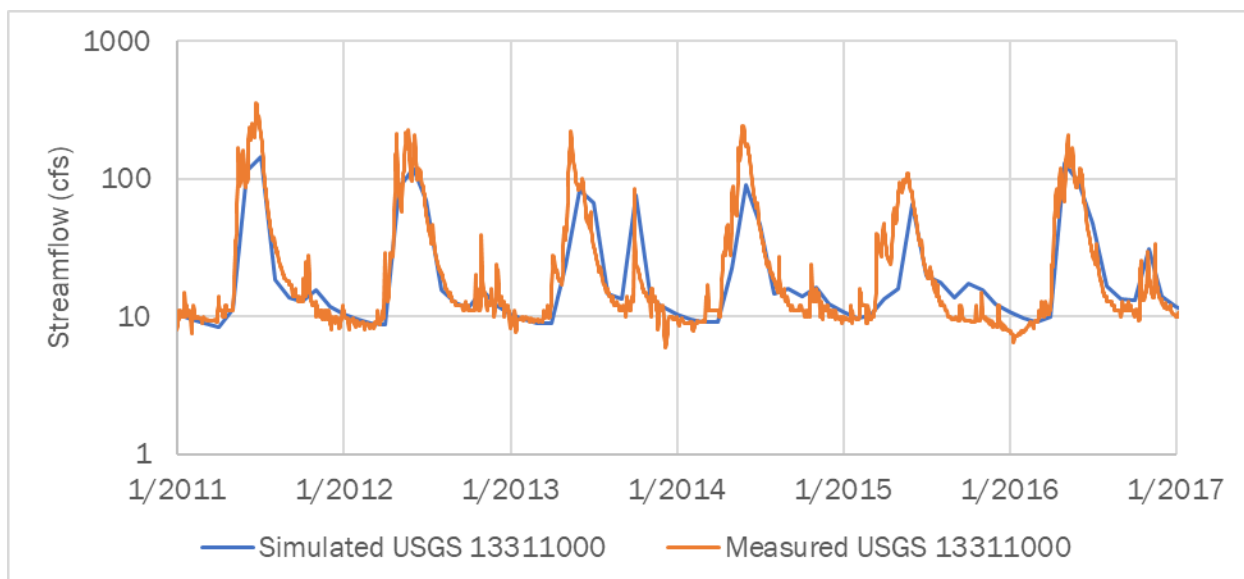
Graph 5-4. Measured vs. simulated flow at USGS gaging station 13310850, Meadow Creek near Stibnite, ID (linear)



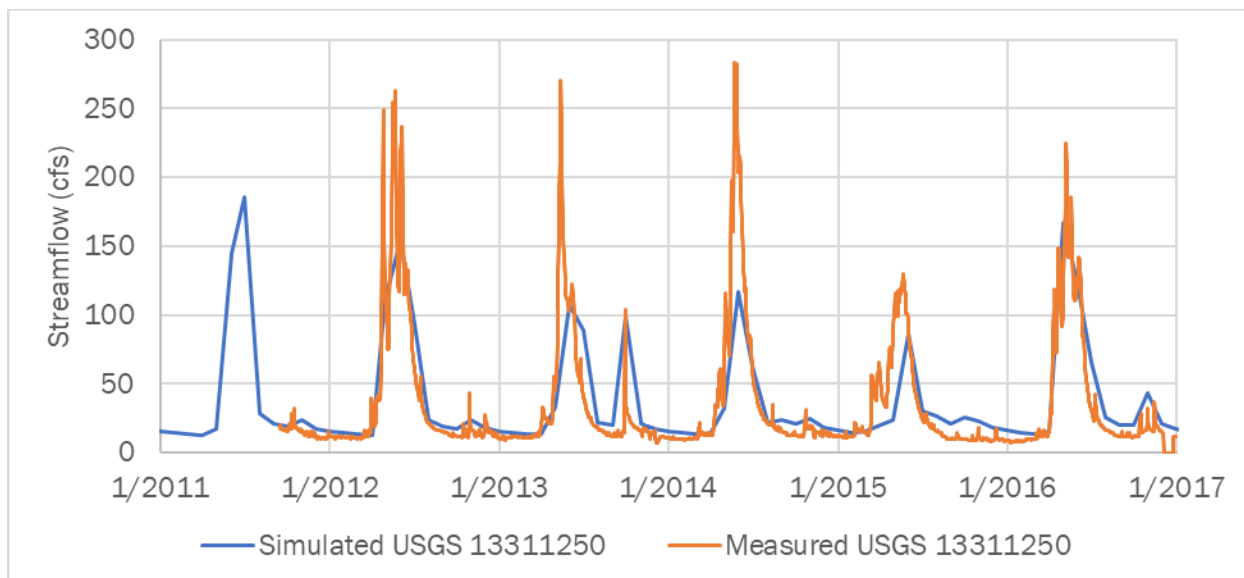
Graph 5-5. Measured vs. simulated flow at USGS gaging station 13310850, Meadow Creek near Stibnite, ID (logarithmic)



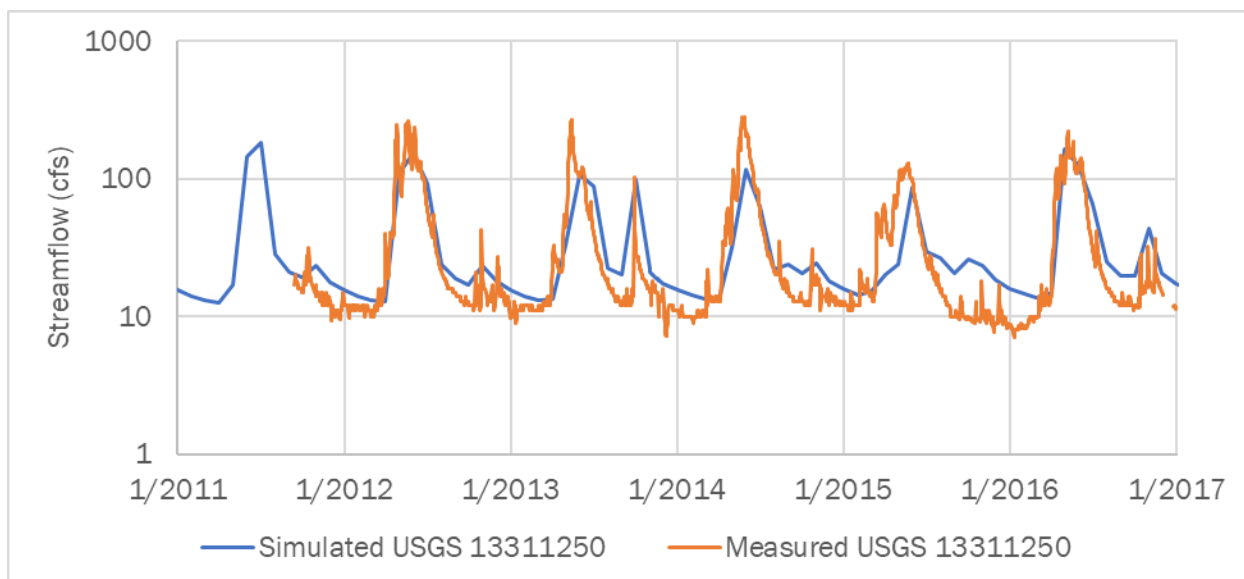
Graph 5-6. Measured vs. simulated flow at USGS gaging station 13311000, EFSFSR at Stibnite (linear)



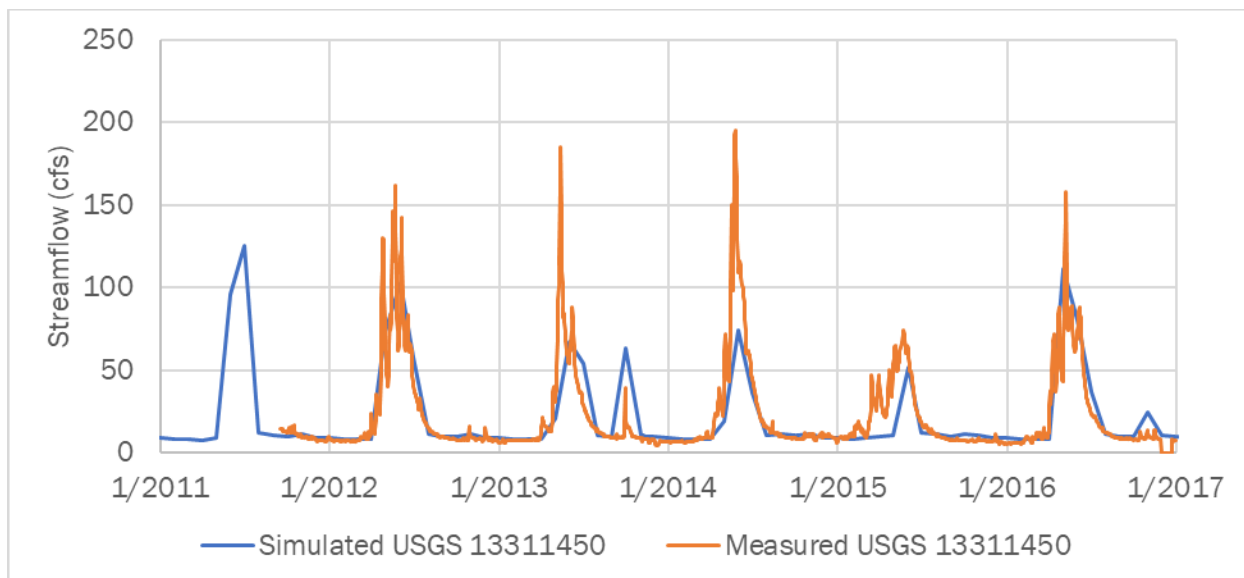
Graph 5-7. Measured vs. simulated flow at USGS gaging station 13311000, EFSFSR at Stibnite (logarithmic)



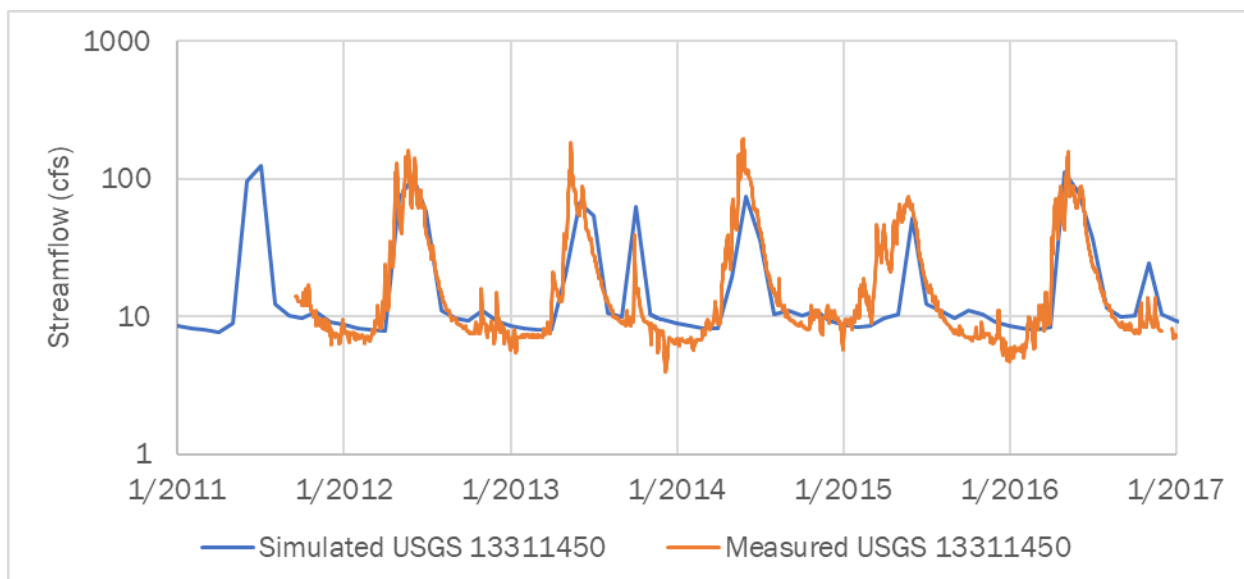
Graph 5-8. Measured vs. simulated flow at USGS gaging station 1331250, EFSFSR above Sugar Creek (linear)



Graph 5-9. Measured vs. simulated flow at USGS gaging station 1331250, EFSFSR above Sugar Creek (logarithmic)



Graph 5-10. Measured vs. simulated flow at USGS gaging station 13311450, Sugar Creek near Stibnite (linear)



Graph 5-11. Measured vs. simulated flow at USGS gaging station 13311450, Sugar Creek near Stibnite (logarithmic)

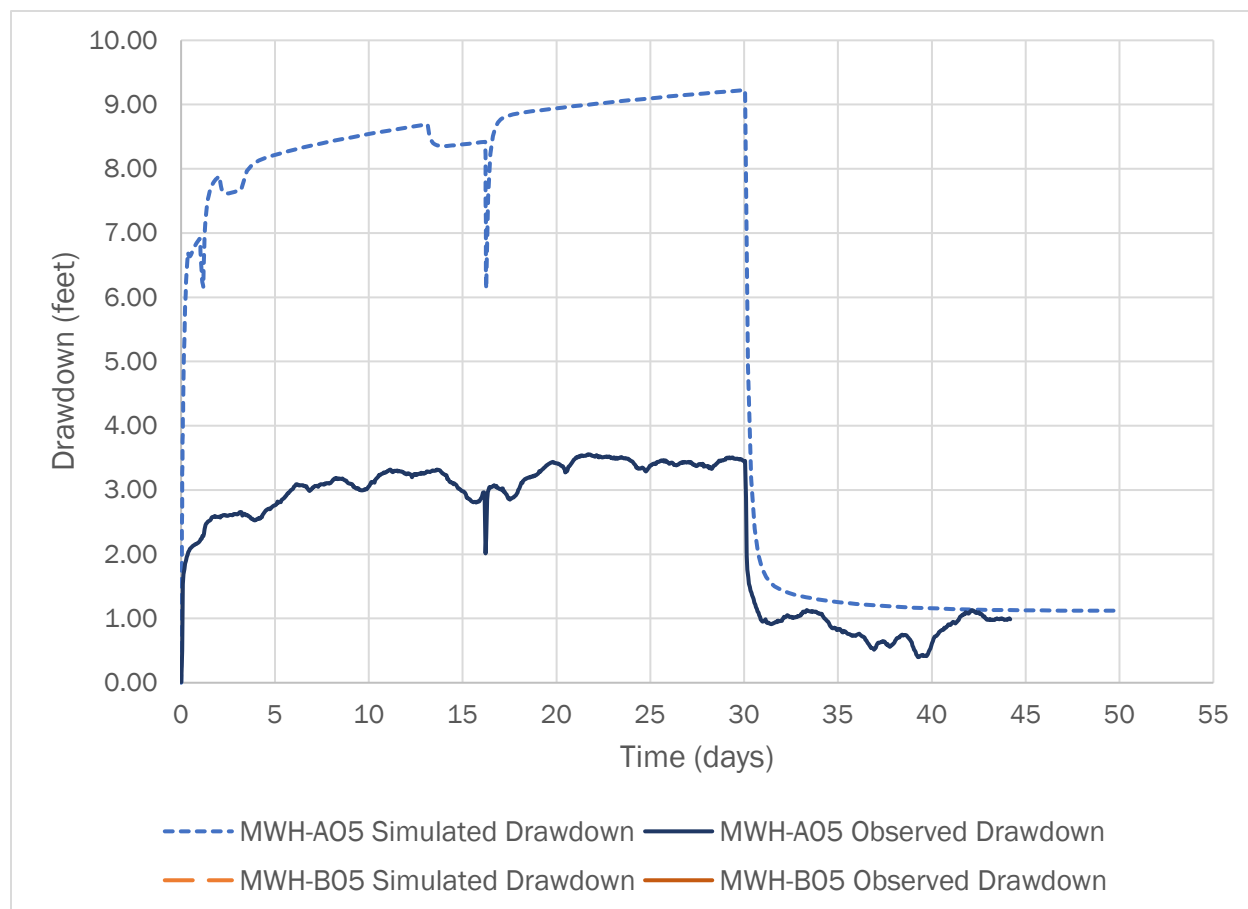
5.4 Gestrin Well Test, December 2013

The existing conditions model calibration represents a balance between simulating seasonal groundwater level fluctuations, observed groundwater levels, and observed surface water flows at a regional scale. The model was also used to simulate the Gestrin well test performed in December 2013. The layer structure used in existing conditions model is a poor analog of test conditions. The Gestrin well was only screened over a 10-ft interval within alluvium at a depth of 100–110 ft below ground surface (bgs). Aquifer responses were observed in monitoring wells also with 10-ft screen intervals, with alluvial monitoring wells generally screened at depths 30–40 ft bgs near the water

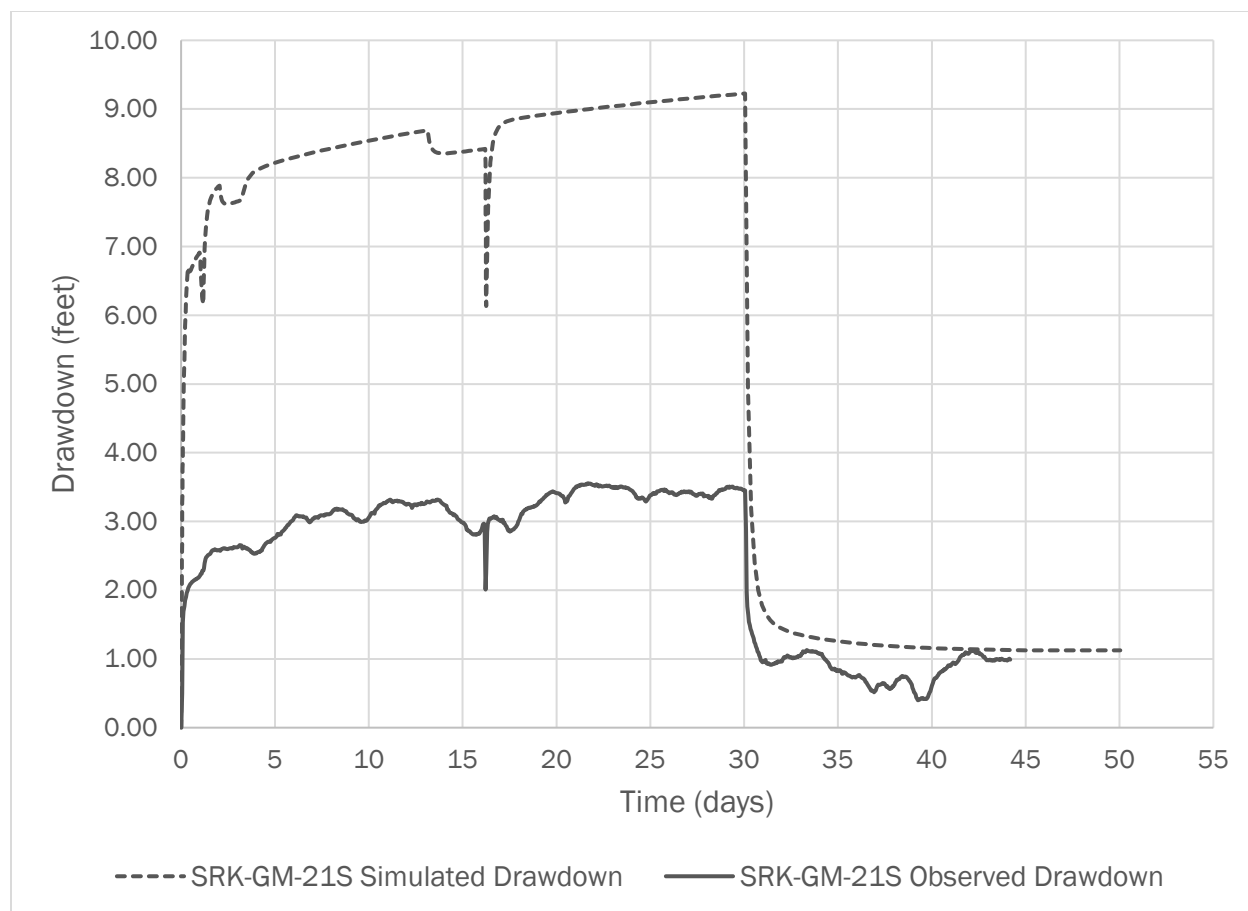
table, and bedrock wells generally screened at depths 230–240 ft bgs in the upper bedrock. Model Layer 1, representing alluvium, is approximately 190 ft thick near the pumping well. In the model, this pumping is simulated by extraction from the entire 190-ft interval of Layer 1, which is not directly analogous to pumping from an isolated 10-ft interval.

In addition, results of the pumping test show the influence of local heterogeneity, indicative of a linear zone or compartment parallel to Meadow Creek, which results in drawdowns from the test extending from approximately 1,400 ft upgradient of the pumping well to approximately 2,000 ft downgradient of the pumping well. Model testing indicates that addition of a thin, local-scale permeable zone linking the upgradient and downgradient areas is required to match aquifer test results. However, the presence of such a zone is not corroborated by other data (e.g., borehole logs, geophysics, etc.), nor is it extensive enough to impact regional-scale dewatering or pit inflow simulations. Therefore, the existing conditions model was not calibrated to the far-field responses observed during the test along the linear feature, but rather focused on simulating near-field responses in monitoring wells MWH-A05, MWH-B05, and SRK-GM-21S.

Results of the simulation for these wells are shown on Graphs 5-12 and 5-13. In general, the model reasonably simulates near-field responses from the Gestrin well test, especially given the disparity between well construction and the model construction.



Graph 5-12. Measured vs. simulated drawdown in wells MWH-A05 and MWH-B05



Graph 5-13. Measured vs. simulated drawdown in well SRK-GM-21S

Section 6

Discussion and Conclusions

The existing conditions model of the upper watershed of the EFSFSR has been developed and calibrated. It realistically simulates the observed system and reproduces measured surface flows and groundwater levels for the period of record. As such, it is an appropriate tool to be used in subsequent project phases to assess system changes during and after mining, including:

- Estimate dewatering rates required to develop the open pit mines.
- Estimate ranges of surface and groundwater flows at different locations, under different conditions and at different phases of mining and post-closure, to support site-wide water-balance and water-quality modeling.
- Estimate the local effects of dewatering and water management strategies on groundwater levels and stream flows.
- Project post-mining open pit filling and pit water balances.
- Provide water balance inputs to the evaluation of the downstream effects of the Project (potential changes in EFSFSR flow and water quality).

These model applications will be reported separately. An analysis of the sensitivity of different model results to uncertain parameters will be performed to identify a range of potential flow conditions that may be encountered during mining.

Evaluation of potential Project effects on downstream flow and water quality in the EFSFSR will be based on combined results of the hydrologic model, the site-wide water balance model, the site-wide water chemistry model, and the stream/pit lake network temperature model. The flow of information from the different models used to evaluate the effects of the Project is illustrated on Figure 6-1.

Section 7

References

- Anderson, M.P., W.W. Woessner, and R.J. Hunt, 2015, *Applied Groundwater Modeling, Simulation of Flow and Advective Transport*, Second Edition, Elsevier.
- BC (Brown and Caldwell), 2017, *Stibnite Gold Project Water Resource Baseline Summary Report*, prepared for Midas Gold Idaho, Inc., June 2017.
- Daly, C., Halbleib, M., Smith, J.I., Gibson, W.P., Doggett, M.K., Taylor, G.H., Curtis, J., and Pasteris, P.A., 2008, *Physiographically-sensitive mapping of temperature and precipitation across the conterminous United States: International Journal of Climatology*, DOI: 10.1002/joc.1688.
- HydroGeo, Inc., 2012, *Surface water hydrology baseline study for Golden Meadows project*, prepared by HydroGeo, Inc. for Midas Gold Inc., December 2012.
- Jones, M.A., 2006, *Modelo Hidrológico de la Cuenca del Río Estrecho*, consultant's report prepared by Michael A. Jones for Proyecto Pascua-Lama Compañía Minera Nevada, January 2006.
- JSAI (John Shomaker & Associates, Inc.), 2017, *Final Work Plan: Hydrologic Model of the Upper Watershed of the East Fork of the South Fork of the Salmon River, Stibnite, Idaho*, prepared for Midas Gold Idaho, Inc., October 2017.
- McDonald Morrissey Associates, 1998, *Regional hydrologic model*, consultant's report prepared for Barrick Goldstrike Mines, Inc.
- Midas Gold Idaho, Inc., 2016, *Plan of Restoration and Operations, Stibnite Gold Project, Valley County, Idaho*, September 2016.
- Niswonger, R.G., S. Panday, and M. Ibaraki, 2011, *MODFLOW-NWT, A Newton Formulation for MODFLOW-2005, United States Geological Survey Techniques and Methods 6-A37, Chapter 37 of Section A, Groundwater Book 6, Modeling Techniques*.
- SPF (SPF Water Engineering), 2017. *Final Groundwater Hydrology Baseline Study, Stibnite Gold Project*, prepared for Midas Gold Idaho, Inc., June 2017.
- Stewart, D.E., E.D. Stewart, R.S. Lewis, K.N. Weppner, and V.H. Isakson, 2016, *Geologic Map of the Stibnite Quadrangle, Valley County, Idaho. Idaho Geologic Survey, Geologic Map 51, 2 sheets, Scale 1:24,000*.

Section 8

Figures

Figure 1-1. Location Map of the Stibnite Gold Project, Valley County, Idaho

Figure 1-2. Proposed Stibnite Gold Project Mine Features

Figure 2-1. EFSFSR Streams and Basins

Figure 2-2. USGS Surface Flow Gaging Stations

Figure 2-3. Groundwater Monitoring Locations

Figure 2-4. Alluvial Groundwater Elevations and Contours—Fall 2015

Figure 2-5. Thickness of Overburden

Figure 3-1. Schematic Showing Modeling Structure

Figure 4-1. Existing Conditions Model Lateral Extent

Figure 4-2. Existing Conditions Model Grid

Figure 4-3. Extent of Overburden Analysis

Figure 4-4. Cross Section Through Model Row 130

Figure 4-5. Cross Section Through Model Row 60

Figure 4-6. Model Recharge Zones

Figure 4-7. Simulated SFR Segments

Figure 4-8. Model Layer 1 Hydraulic Conductivity

Figure 4-9. Model Layer 2 Hydraulic Conductivity

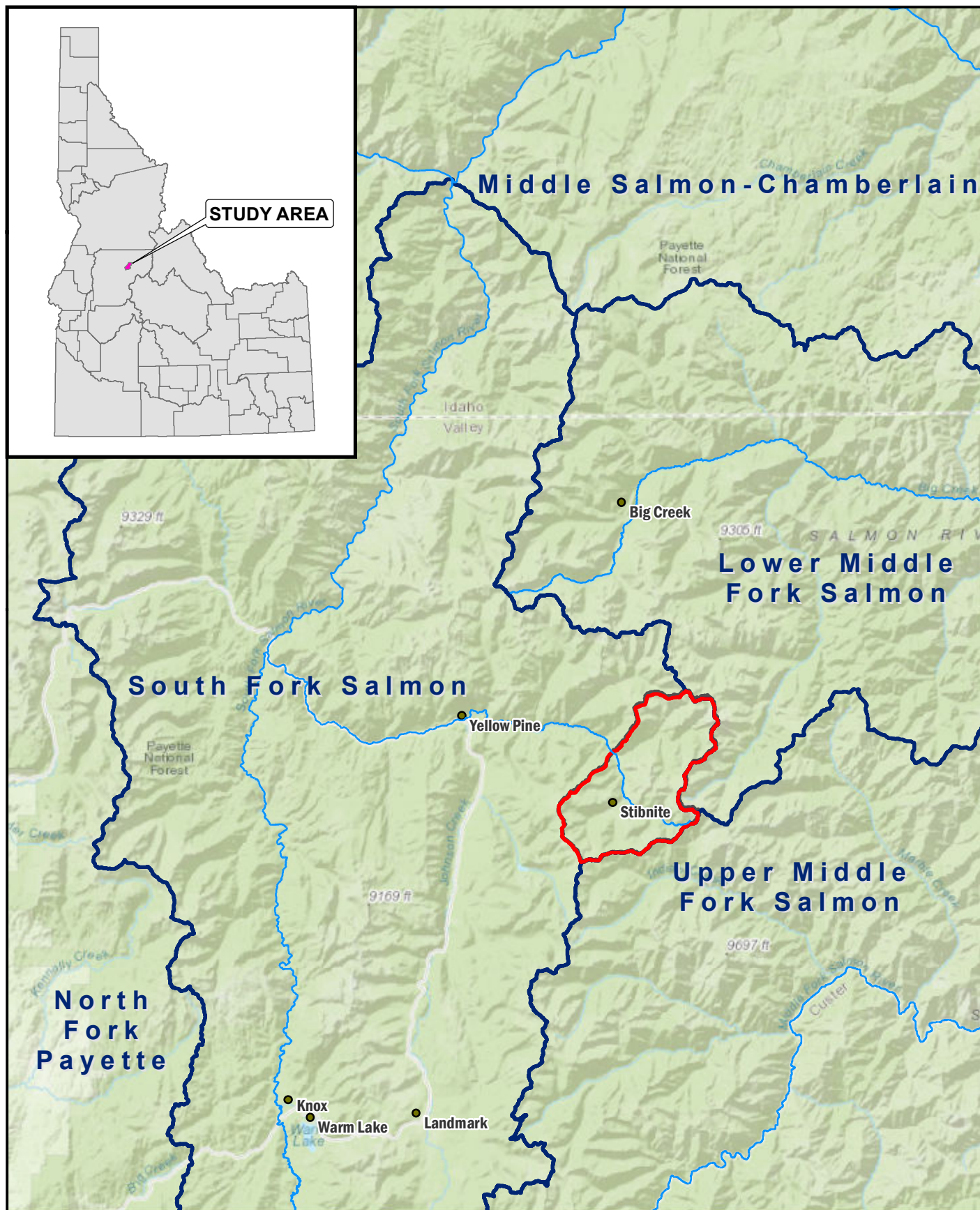
Figure 4-10. Model Layer 2 Specific Yield

Figure 5-1. Simulated Water Table, December 2015

Figure 5-2. Simulated Extent of Saturated Alluvium and Overburden, February 2015

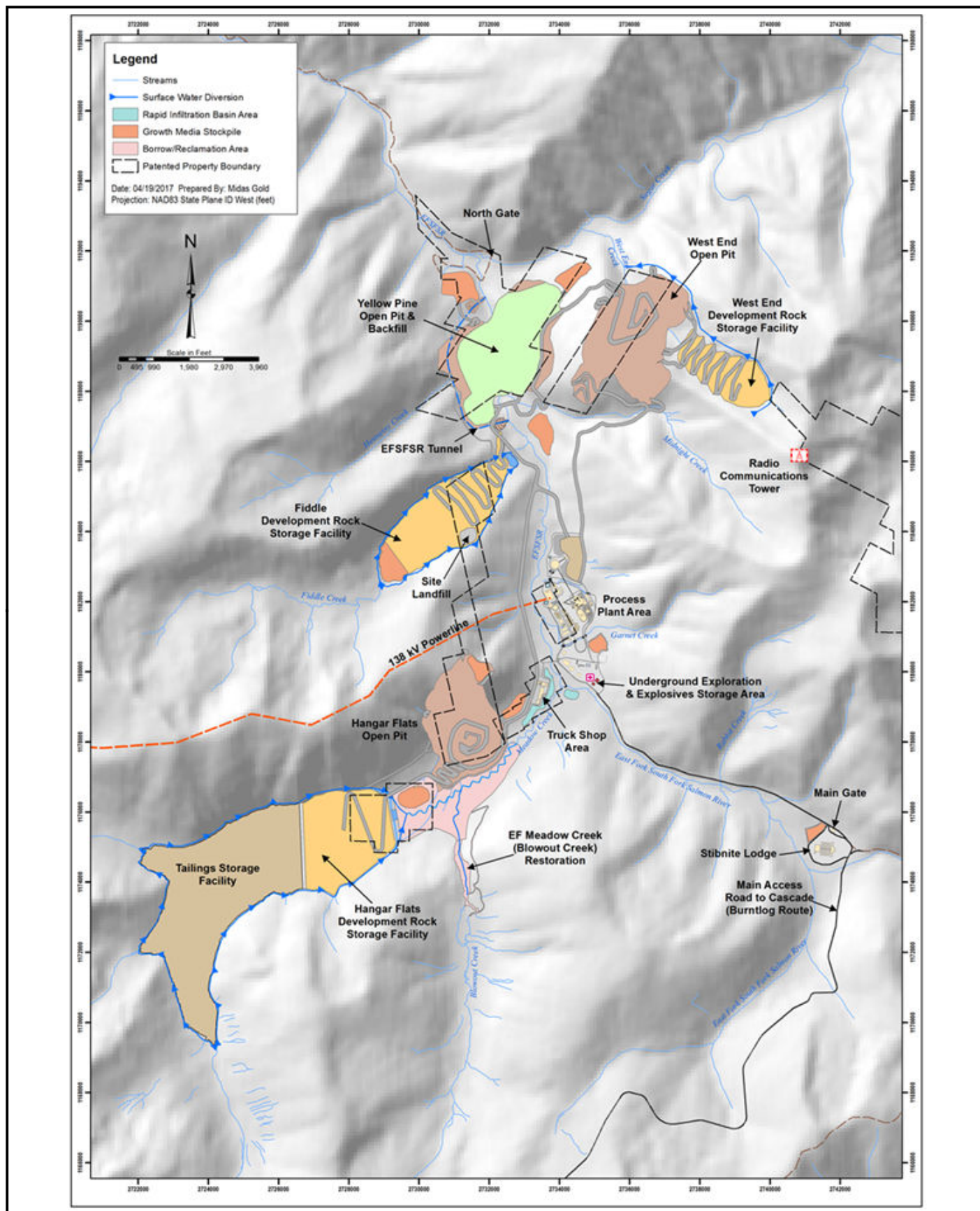
Figure 5-3. Simulated Extent of Saturated Alluvium and Overburden, July 2015

Figure 6-1. Project Modeling Process Diagram



	Date: November 14, 2017	Basemap: Miles	
	Project No: 150696		
	Client: Midas Gold		

Figure 1-1
Location Map of the Stibnite Gold Project, Valley County, Idaho
 Midas Gold Existing Conditions Model
 Stibnite Gold Project

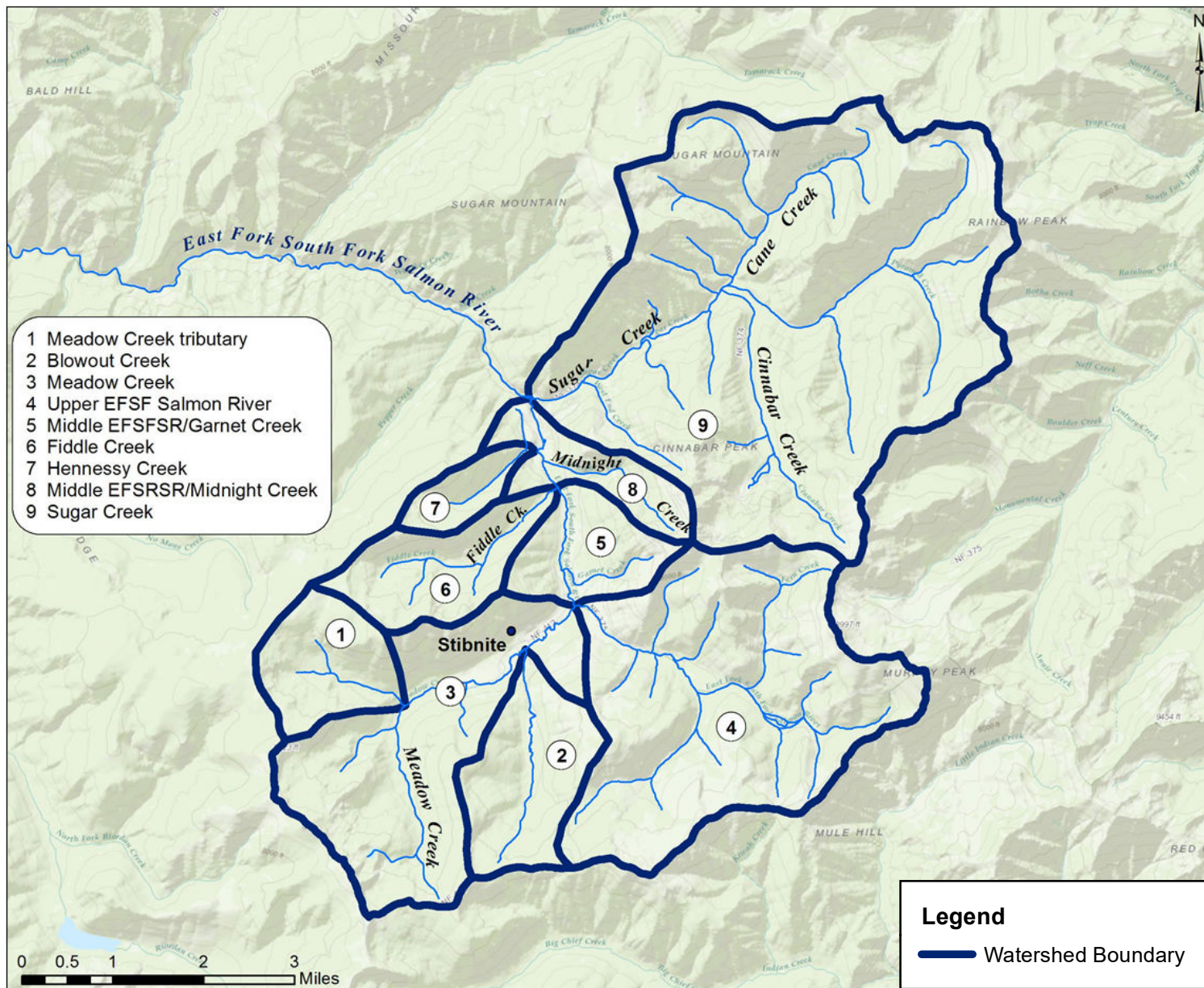


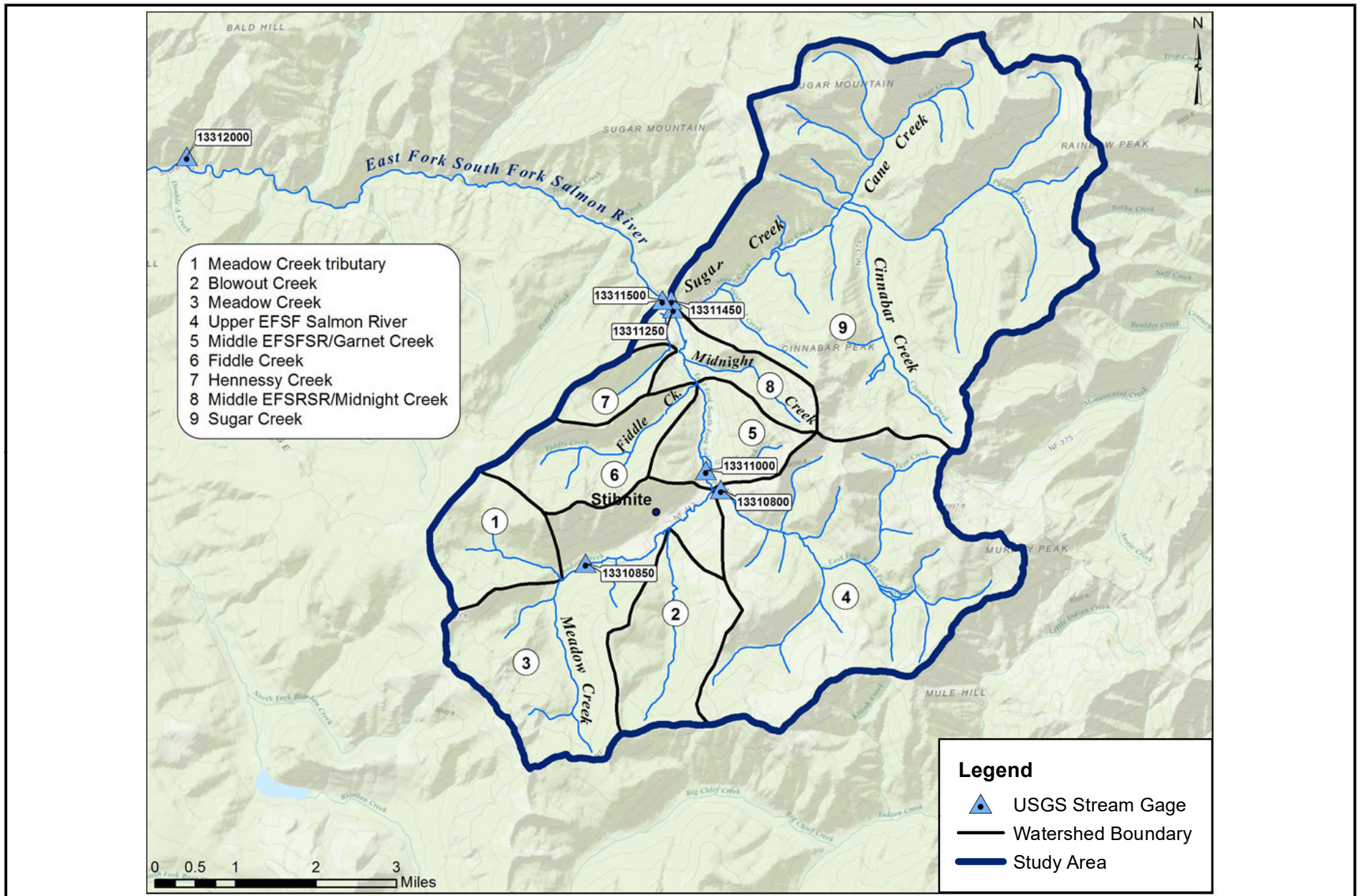
Brown AND Caldwell

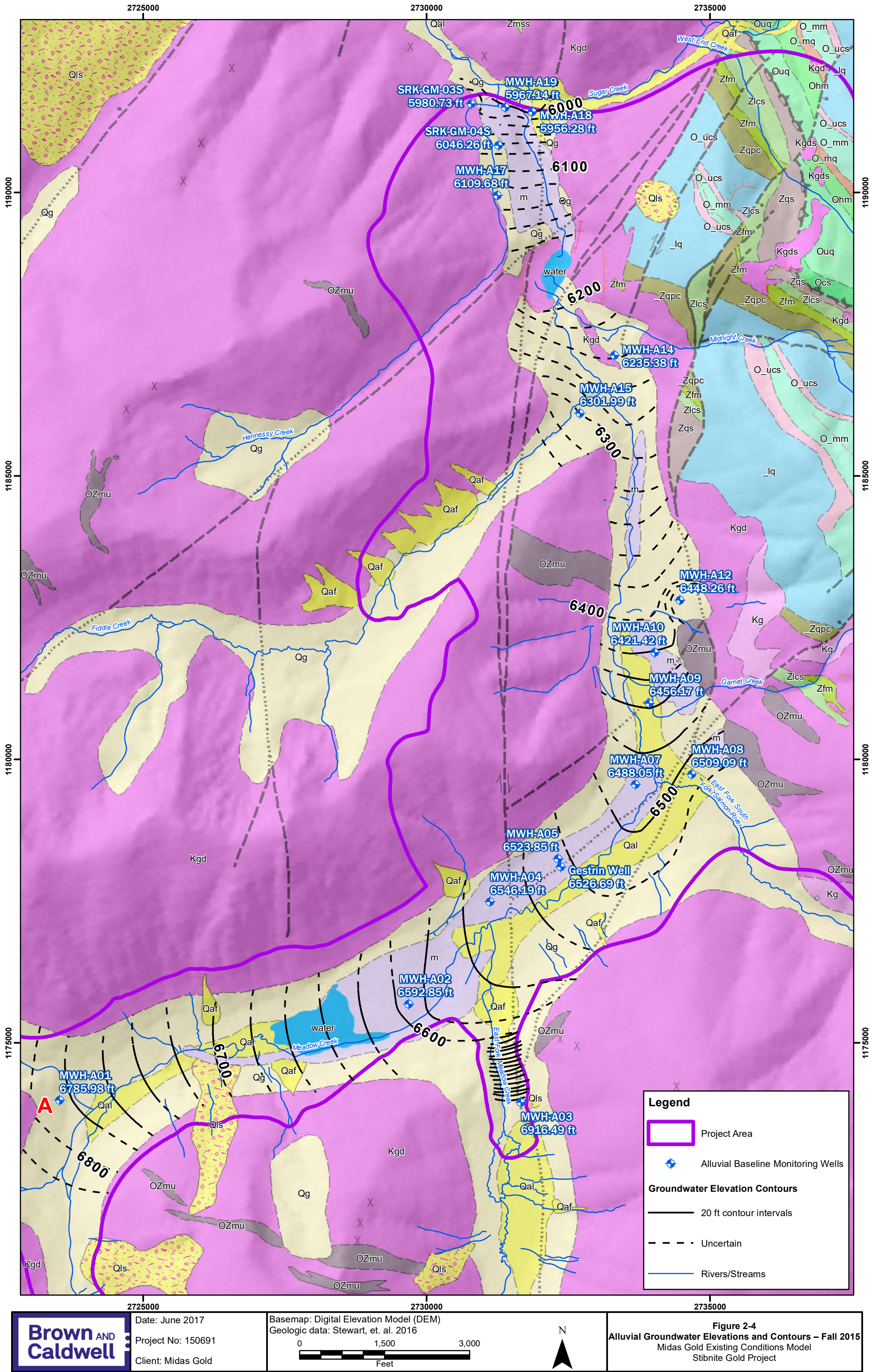
Date: November 14, 2017
Project No: 150696
Client: Midas Gold

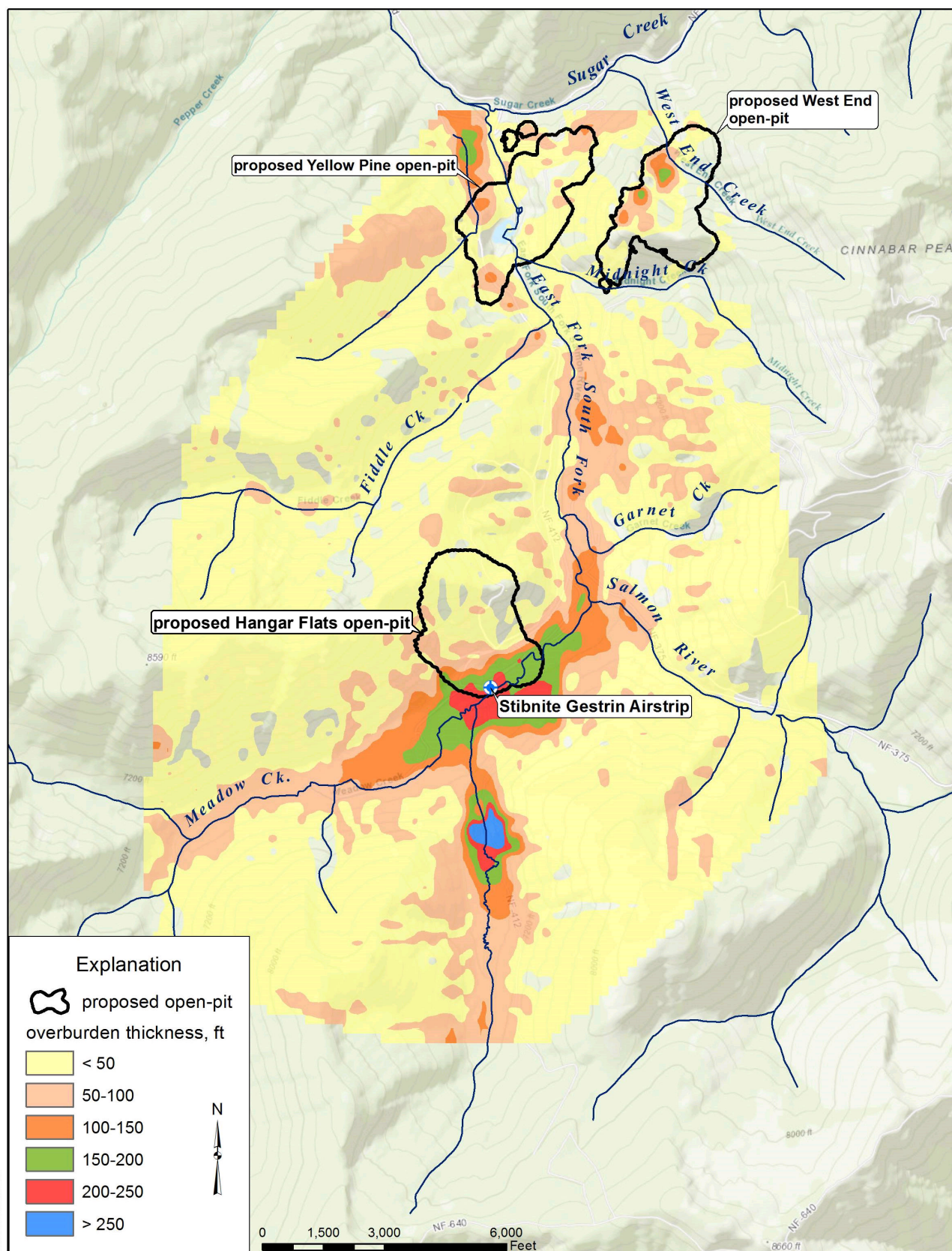
Figure Source: Midas Gold 2016

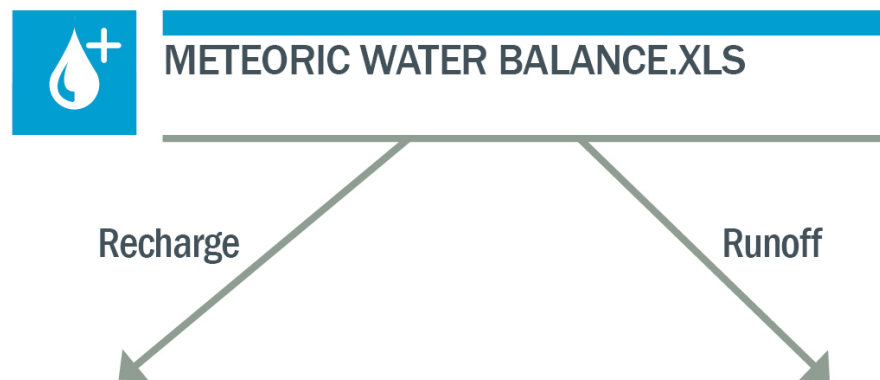
Figure 1-2
Proposed Stibnite Gold Project
Mine Features
Midas Gold Existing Conditions Model
Stibnite Gold Project



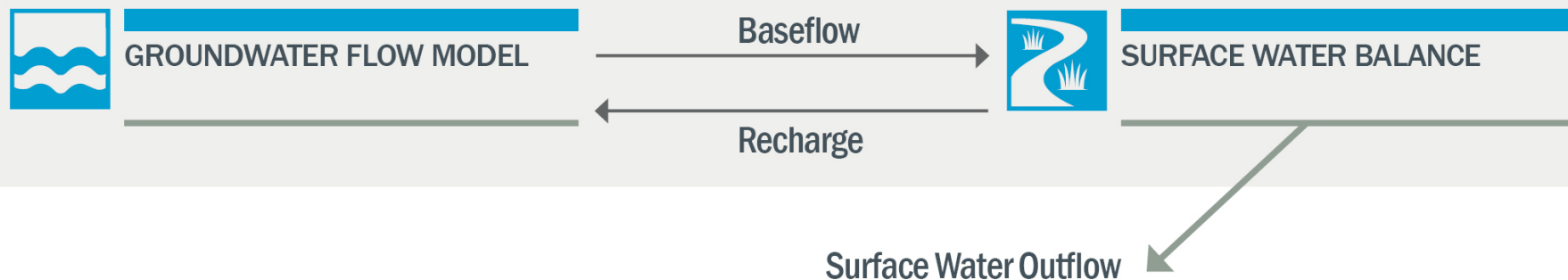


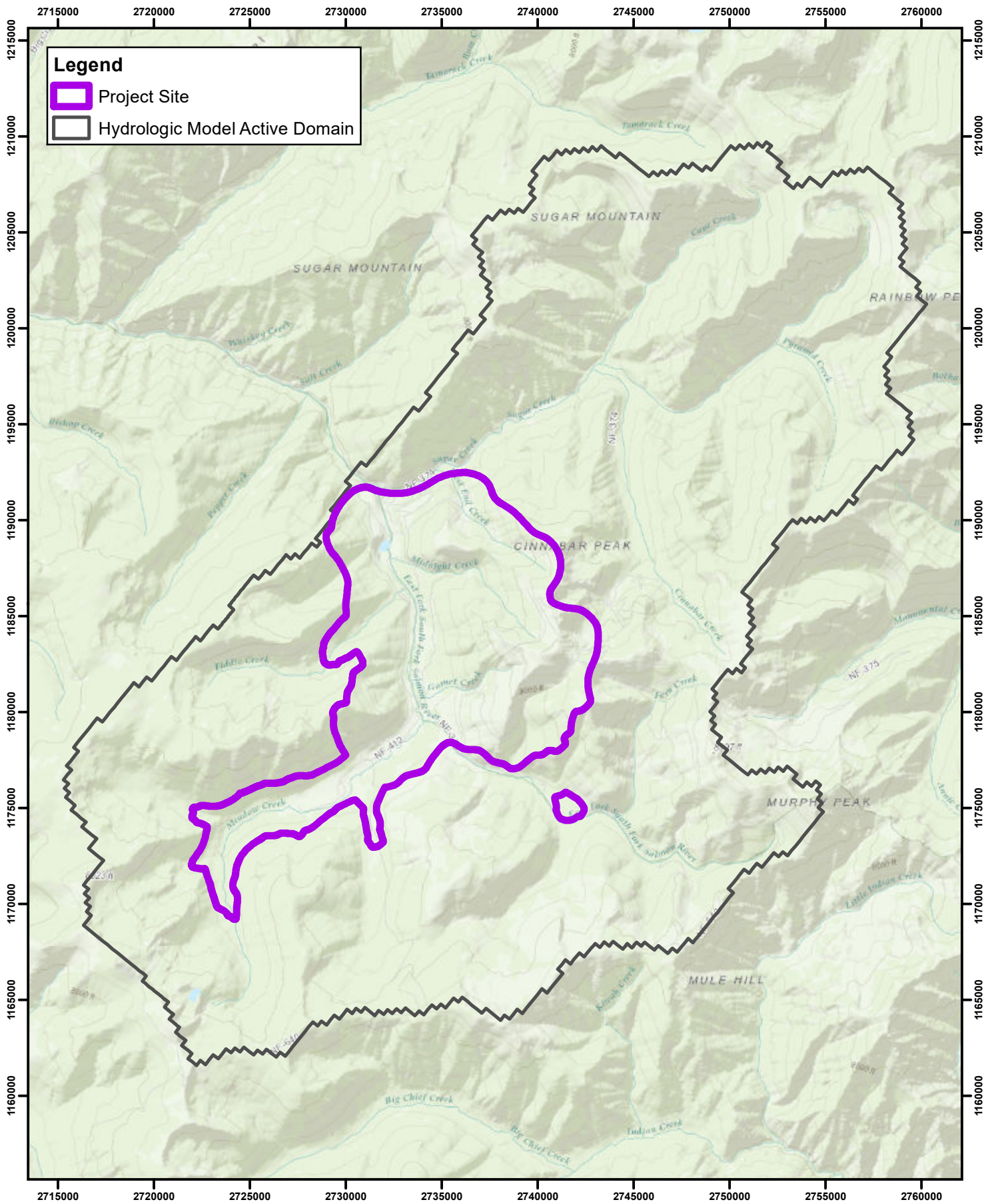



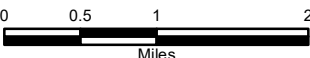



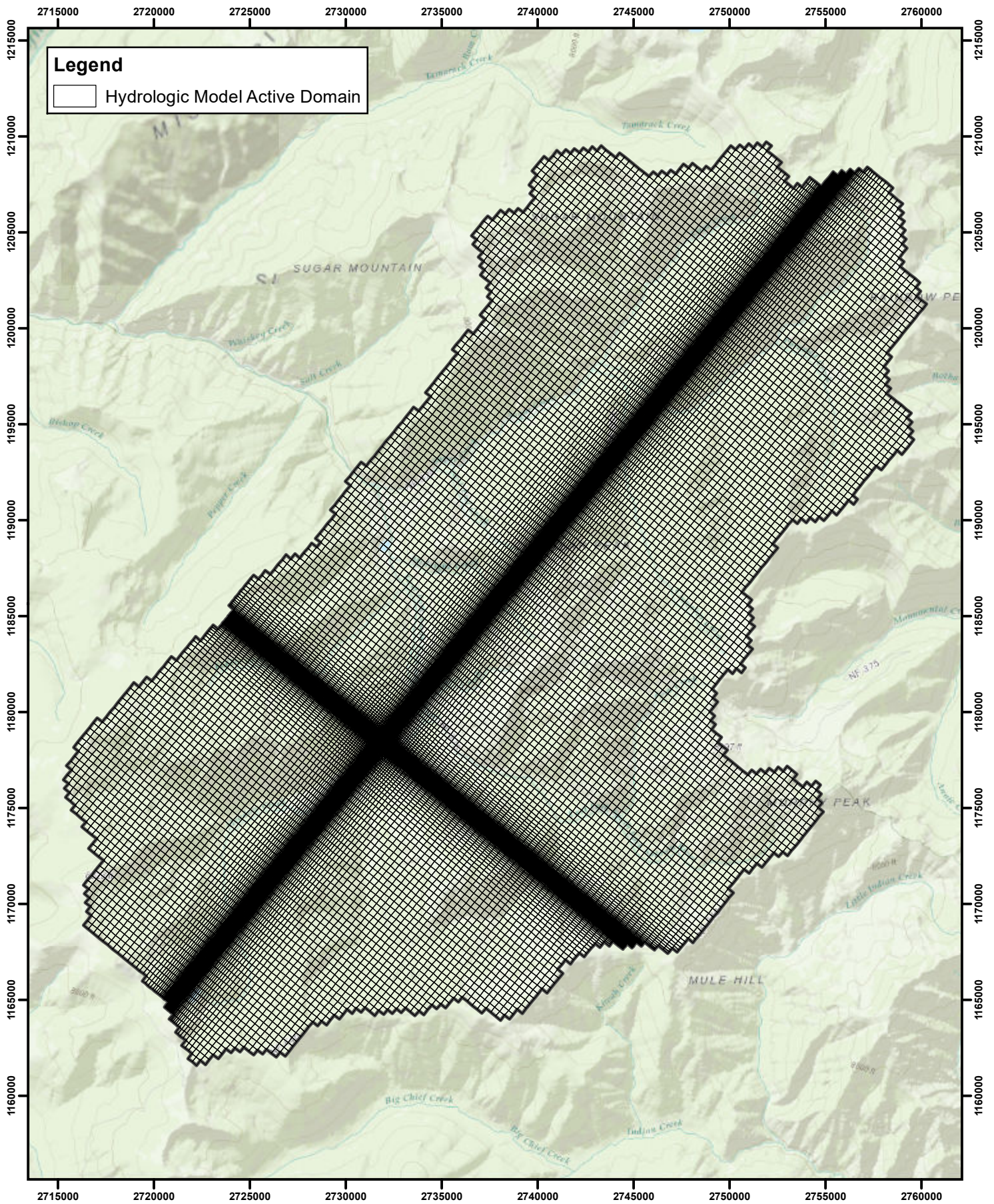



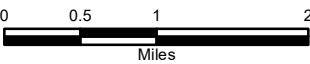

MODFLOW Model

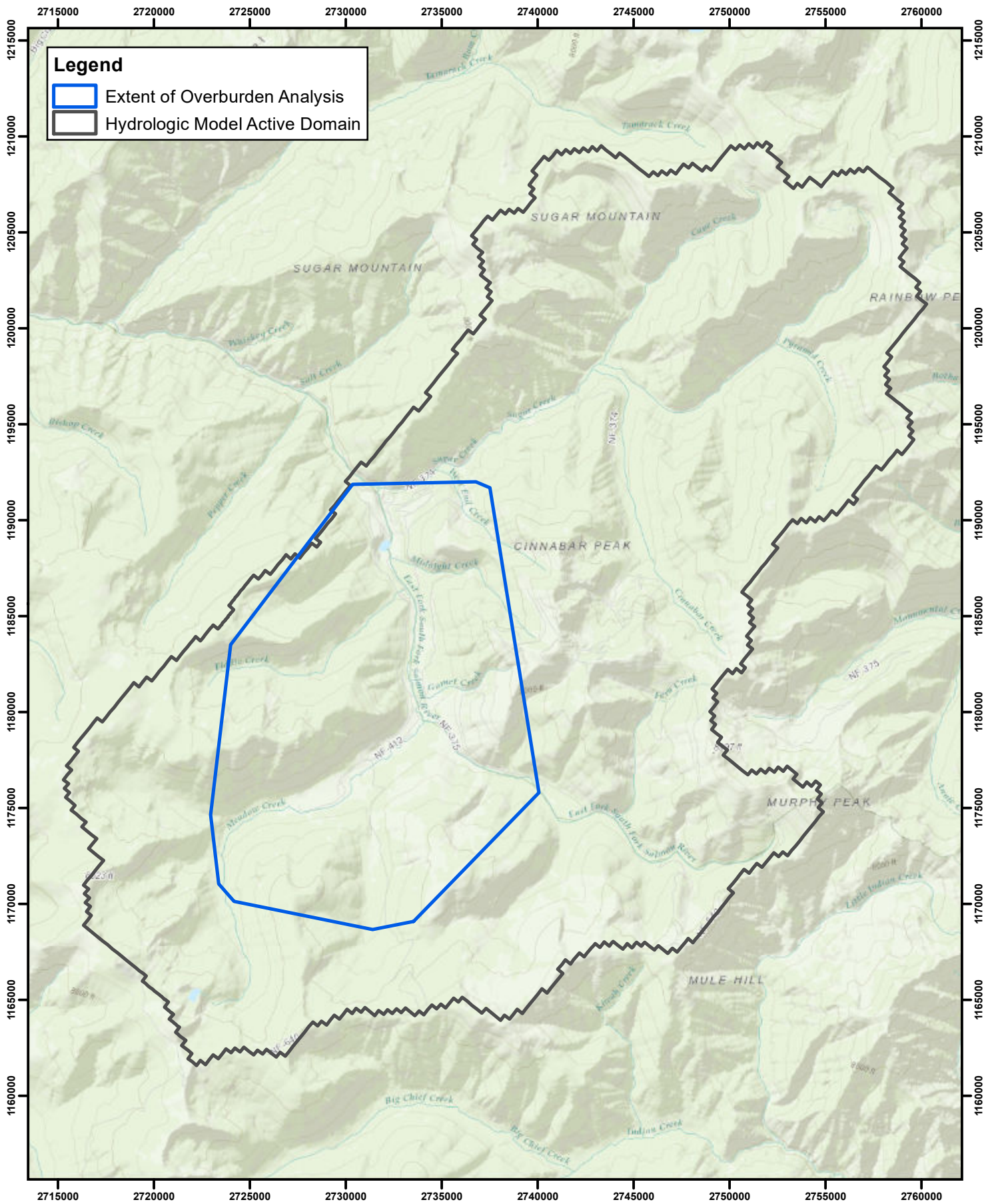




	Date: November 10, 2017	 	Figure 4-1 Existing Conditions Model Lateral Extent Midas Gold Existing Conditions Model Stibnite Gold Project
	Project No: 150696		
	Client: Midas Gold		



	<p>Date: November 10, 2017</p> <p>Project No: 150696</p> <p>Client: Midas Gold</p>	<p>Basemap:</p>  <p>Miles</p> 	<p>Figure 4-2 Existing Conditions Model Grid Midas Gold Existing Conditions Model Stibnite Gold Project</p>
---	--	---	--



Brown AND Caldwell

Date: November 10, 2017
 Project No: 150696
 Client: Midas Gold

Basemap:

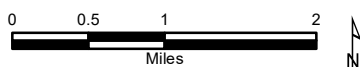
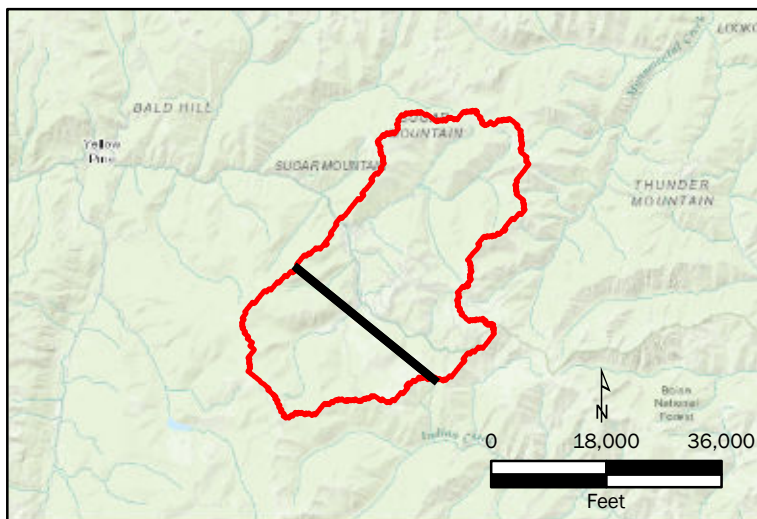
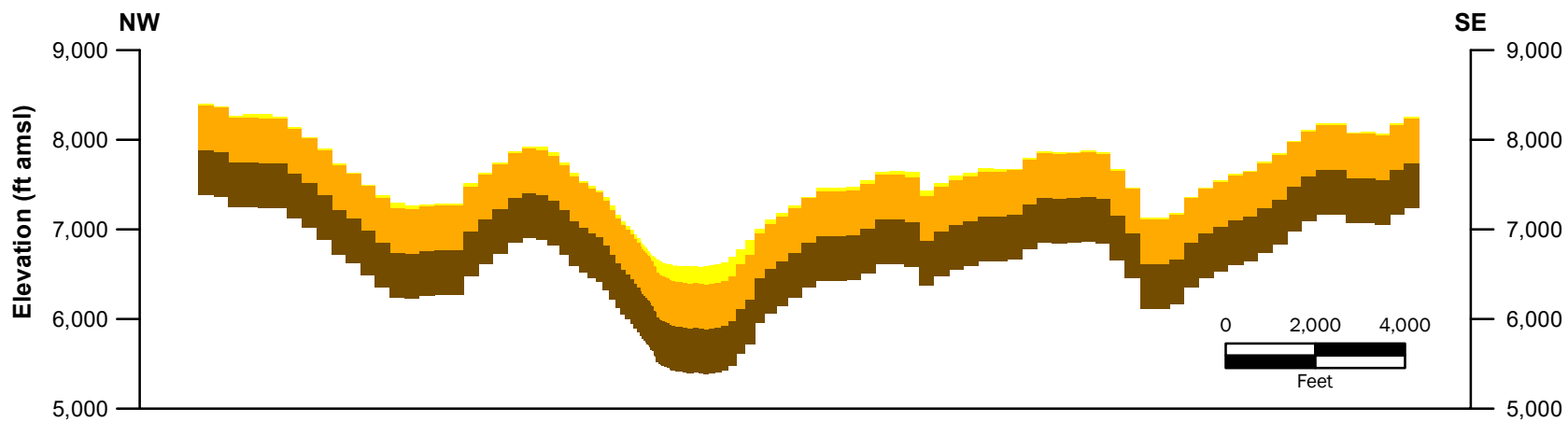


Figure 4-3
Extent of Overburden Analysis
 Midas Gold Existing Conditions Model
 Stibnite Gold Project



Cross-Section Legend

- Model Layer 1
- Model Layer 2
- Model Layer 3

Location Map Legend

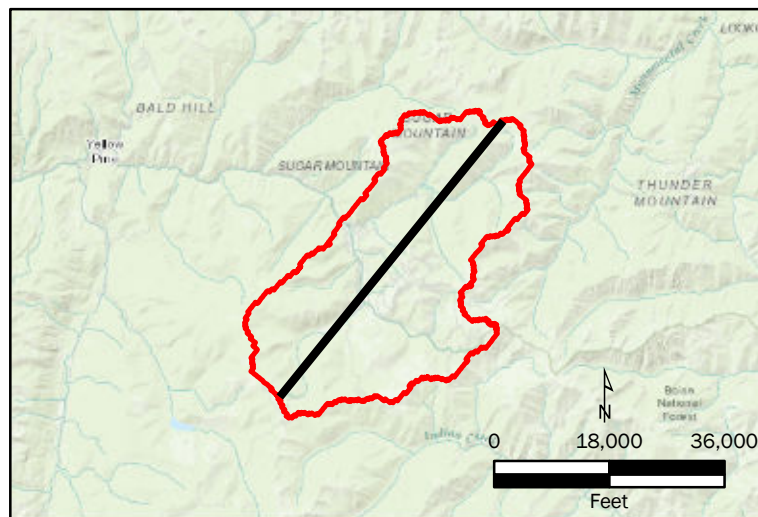
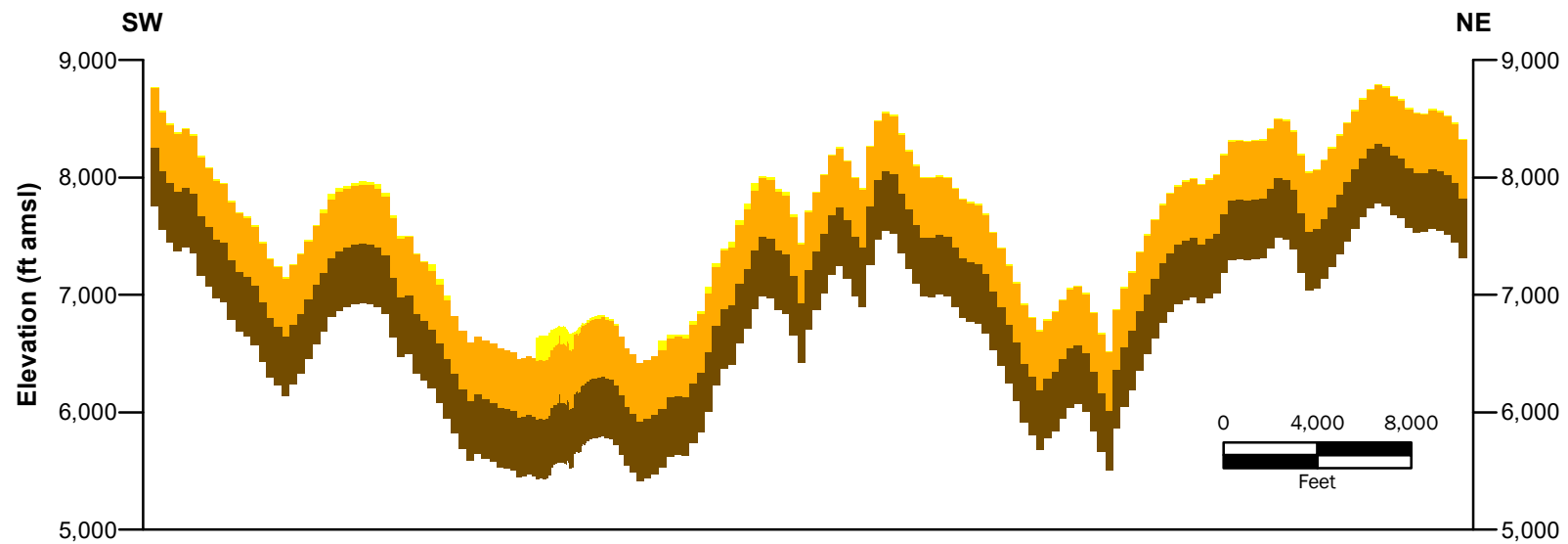
- Cross-Section Line Location
- Hydrologic Model Active Domain

Brown AND Caldwell

Date: November 15, 2017
Project No: 150696
Client: Midas Gold

Note: 2x Vertical Exaggeration

Figure 4-4
Cross Section Through Model Row 140
Midas Gold Existing Conditions Model
Stibnite Gold Project



Cross-Section Legend

- Model Layer 1
- Model Layer 2
- Model Layer 3

Location Map Legend

- Cross-Section Line Location
- Hydrologic Model Active Domain

**Brown AND
Caldwell**

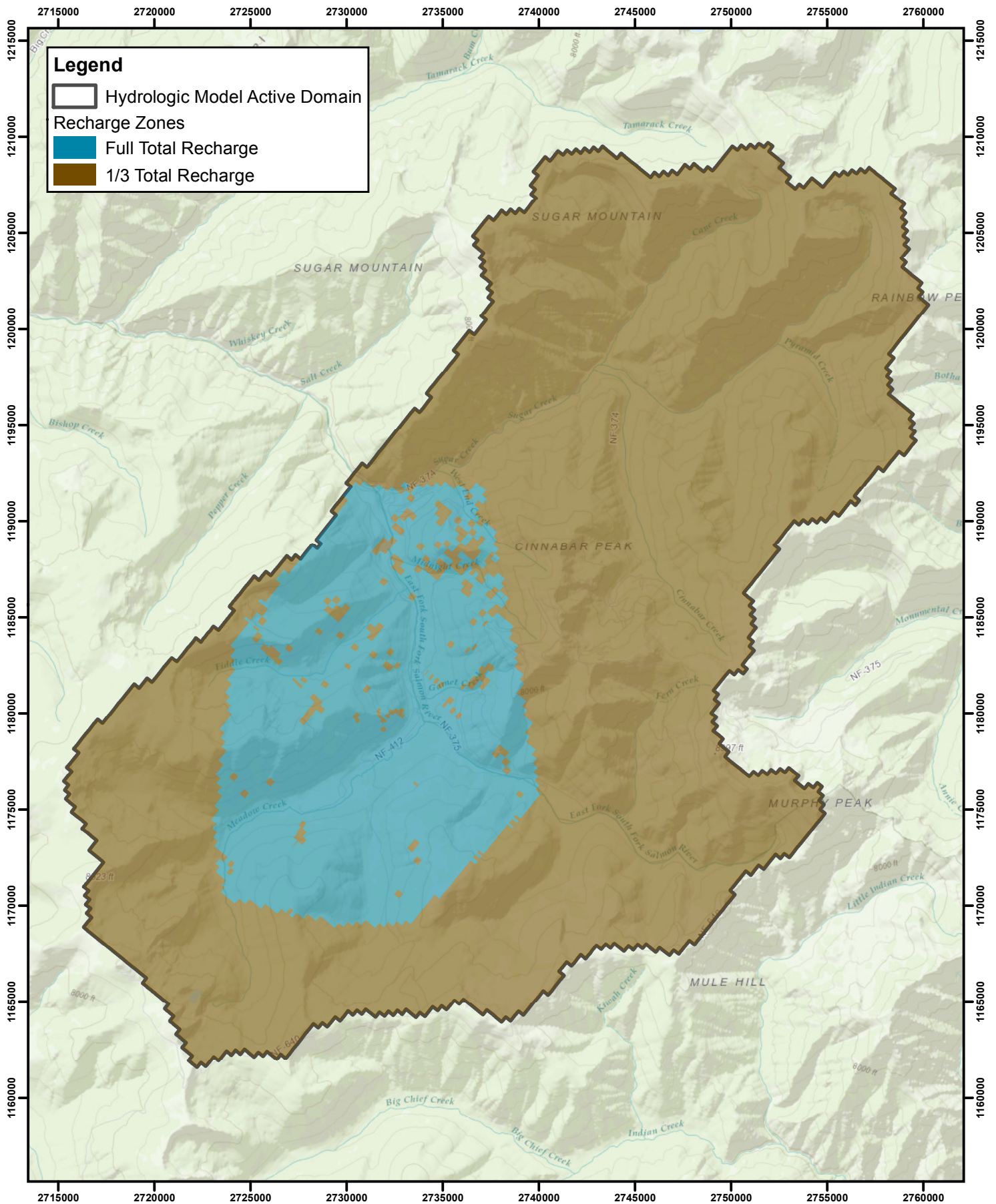
Date: November 15, 2017

Project No: 150696

Client: Midas Gold

Note: 5x Vertical Exaggeration

Figure 4-5
Cross Section Through Model Column 60
Midas Gold Existing Conditions Model
Stibnite Gold Project



Date: November 10, 2017
 Project No: 150696
 Client: Midas Gold

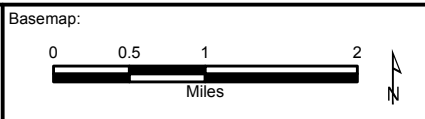
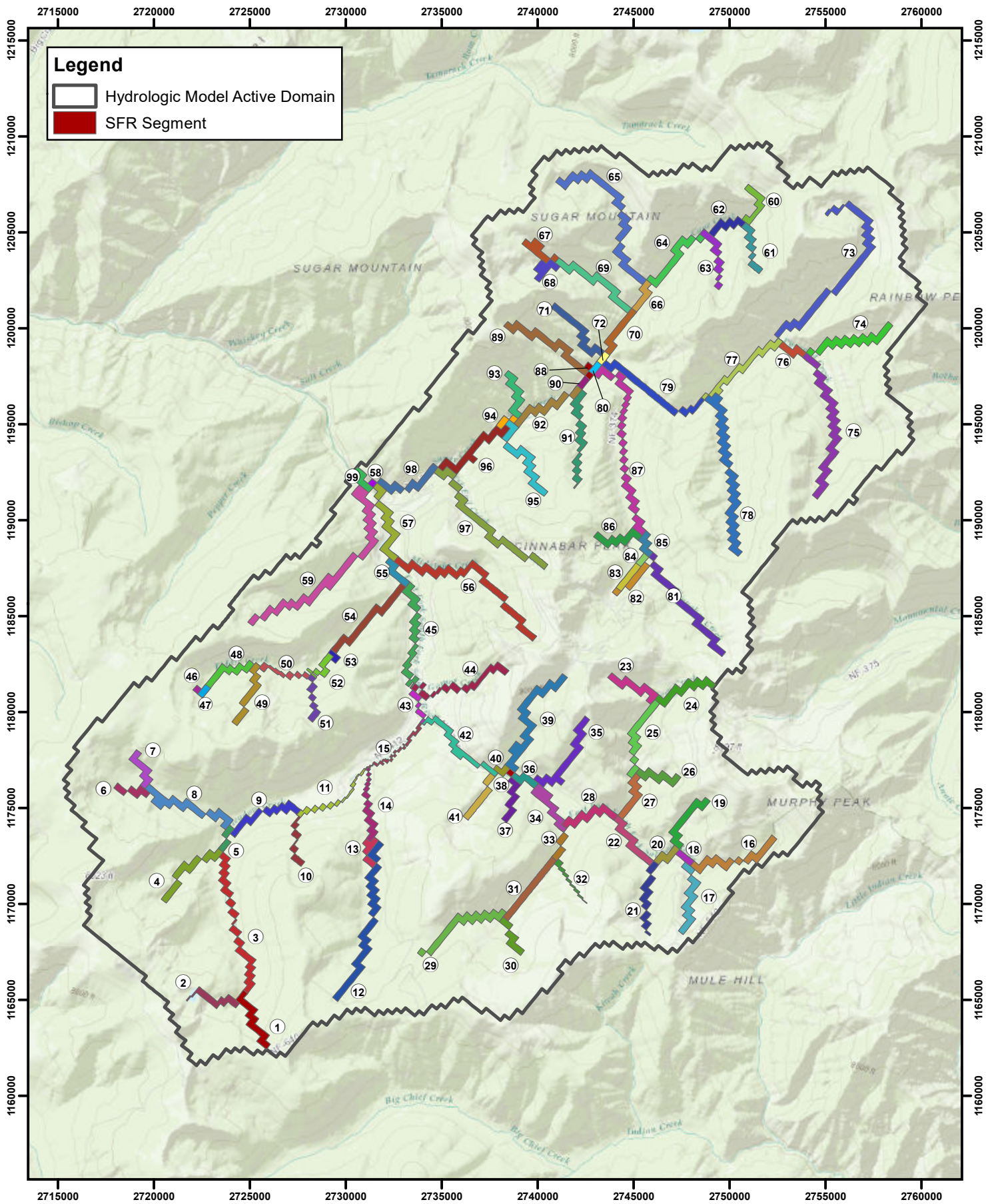


Figure 4-6
Model Recharge Zones
 Midas Gold Existing Conditions Model
 Stibnite Gold Project



**Brown AND
Caldwell**

Date: November 10, 2017
Project No: 150696
Client: Midas Gold

Basemap:

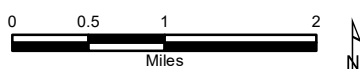
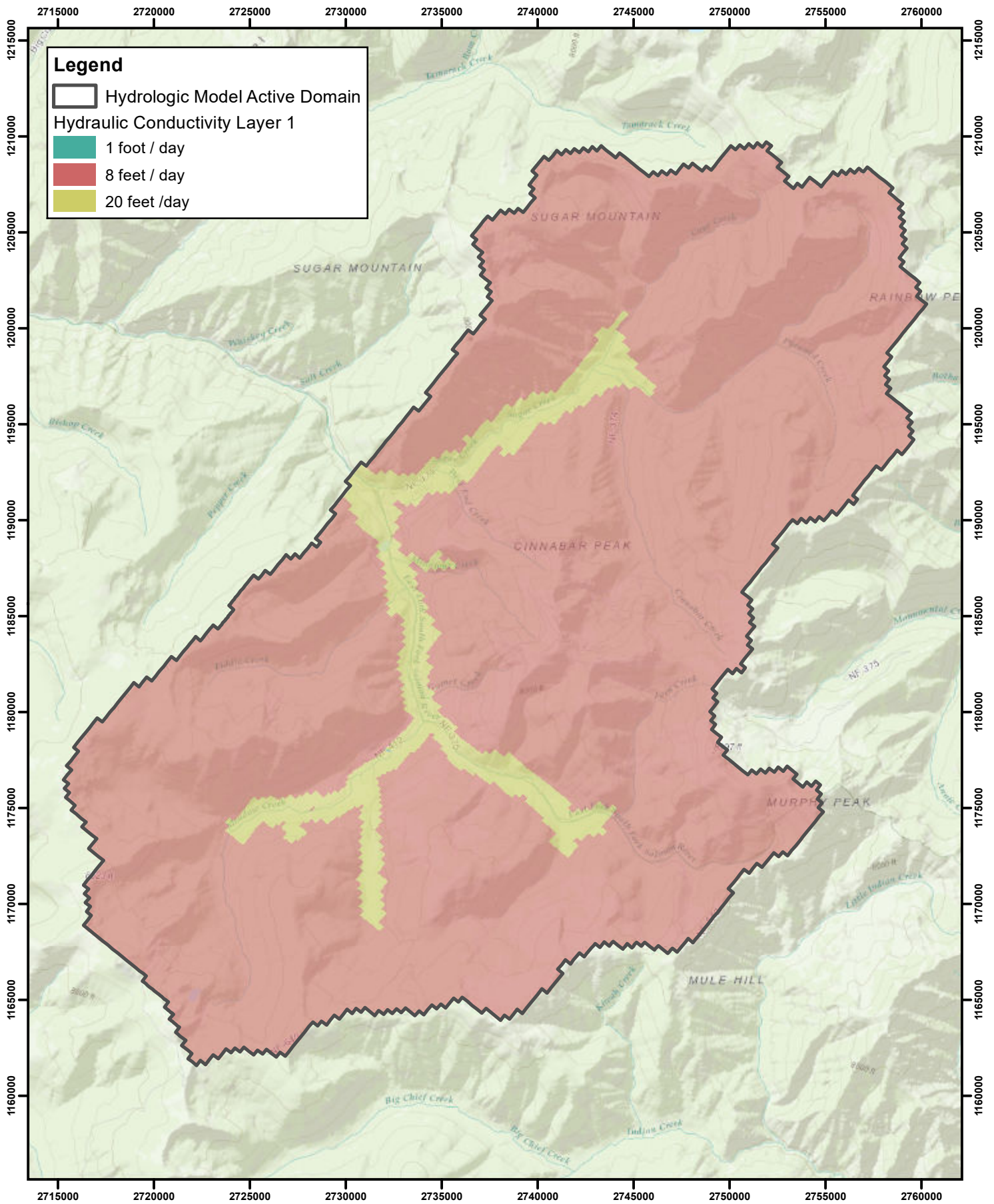


Figure 4-7
Simulated SFR Segments
Midas Gold Existing Conditions Model
Stibnite Gold Project



Brown AND Caldwell

Date: November 10, 2017
 Project No: 150696
 Client: Midas Gold

Basemap:

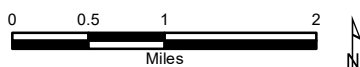
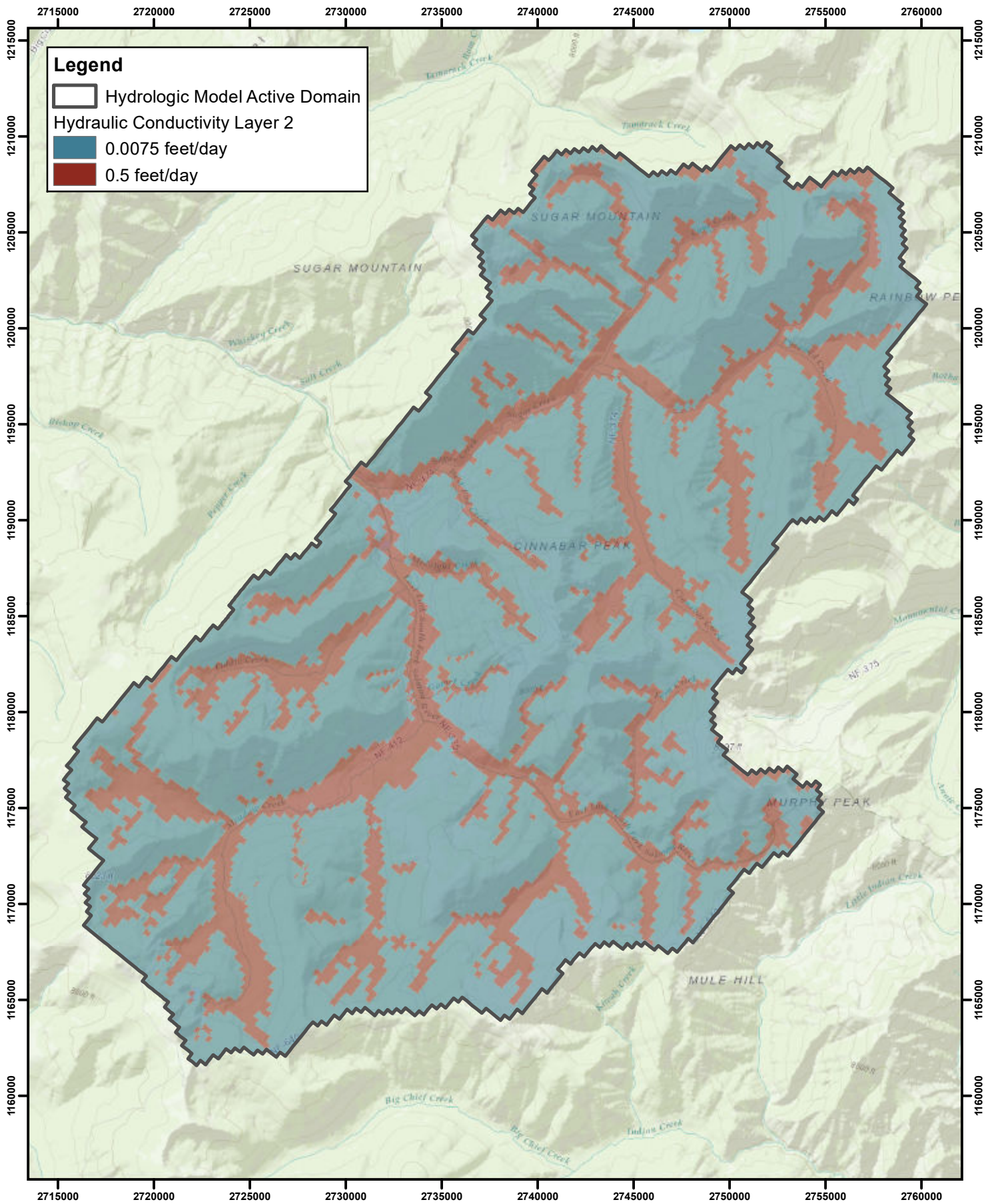


Figure 4-8
Model Layer 1 Hydraulic Conductivity
 Midas Gold Existing Conditions Model
 Stibnite Gold Project



Brown AND Caldwell

Date: November 10, 2017
 Project No: 150696
 Client: Midas Gold

Basemap:

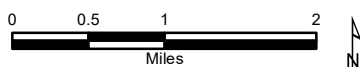
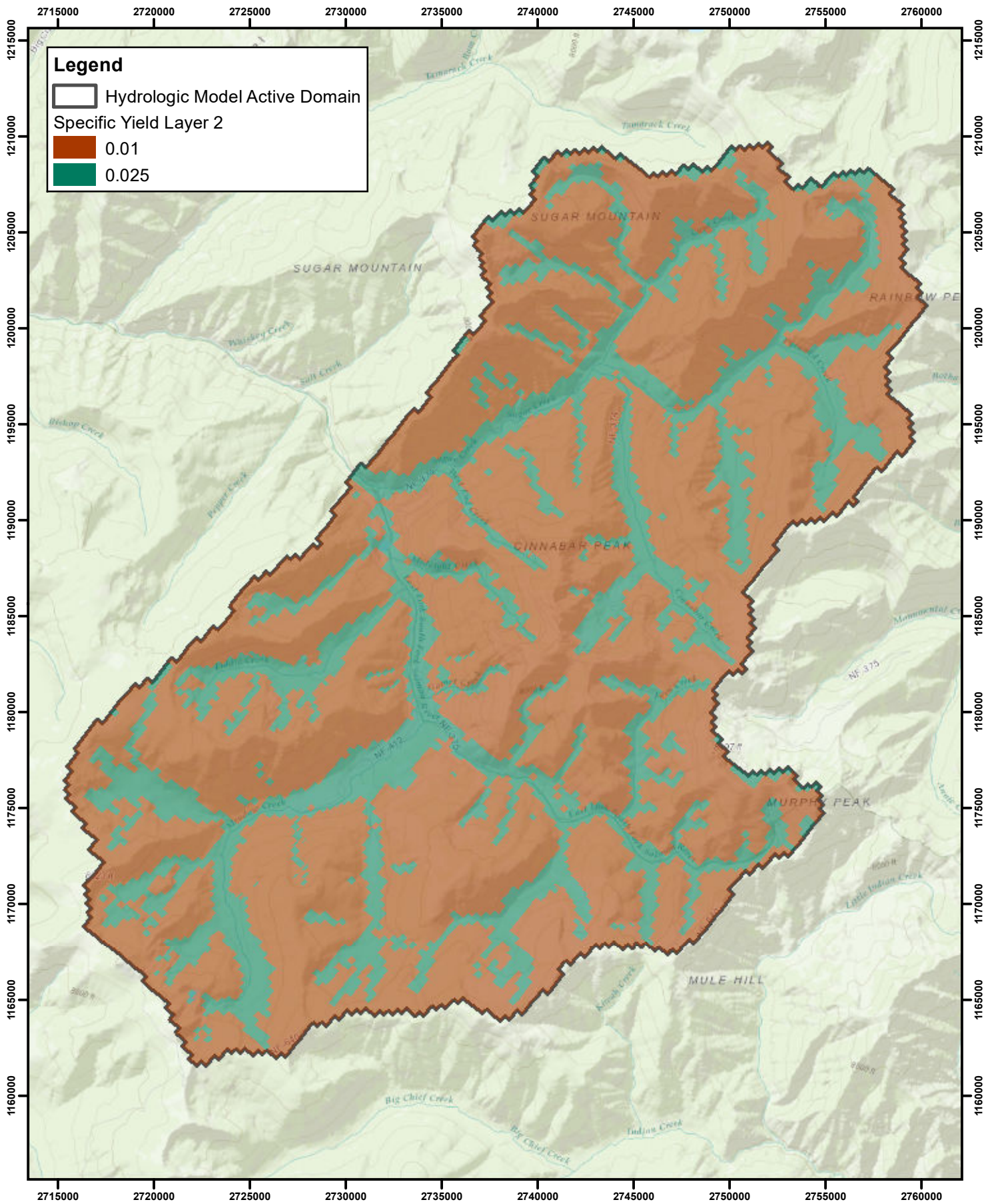


Figure 4-9
Model Layer 2 Hydraulic Conductivity
 Midas Gold Existing Conditions Model
 Stibnite Gold Project



Legend

- Hydrologic Model Active Domain
- Specific Yield Layer 2
 - 0.01
 - 0.025

**Brown AND
Caldwell**

Date: November 10, 2017
Project No: 150696
Client: Midas Gold

Basemap:

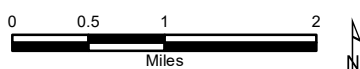
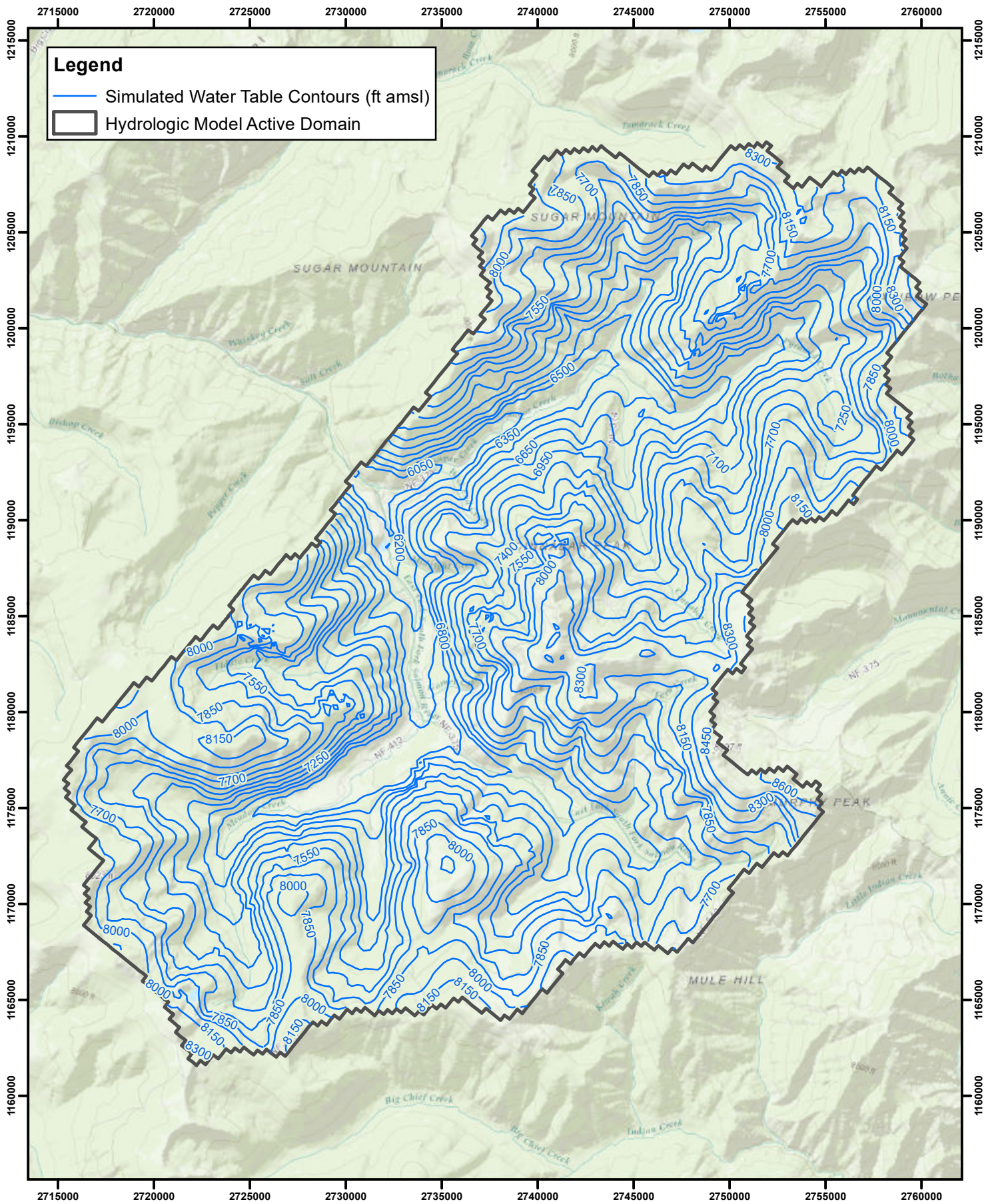

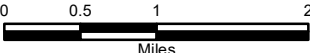

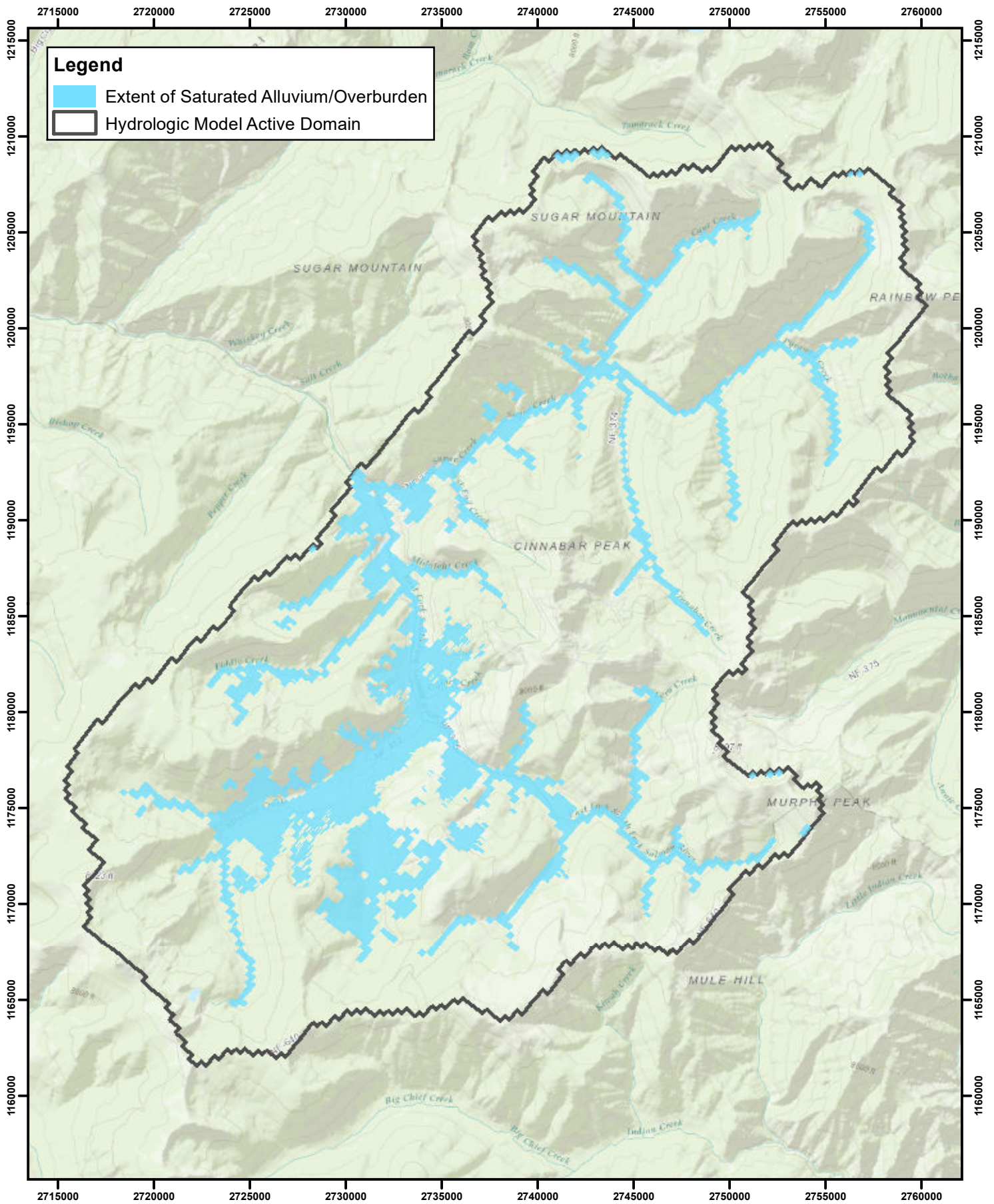


Figure 4-10
Model Layer 2 Specific Yield
Midas Gold Existing Conditions Model
Stibnite Gold Project



	<p>Date: November 10, 2017</p> <p>Project No: 150696</p> <p>Client: Midas Gold</p>	<p>Basemap:</p>  <p>0 0.5 1 2 Miles</p> 	<p>Figure 5-1 Simulated Water Table, December 2015 Midas Gold Existing Conditions Model Stibnite Gold Project</p>
---	--	---	--



Legend

- Extent of Saturated Alluvium/Overburden
- Hydrologic Model Active Domain

Brown AND Caldwell

Date: November 10, 2017
 Project No: 150696
 Client: Midas Gold

Basemap:

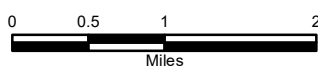
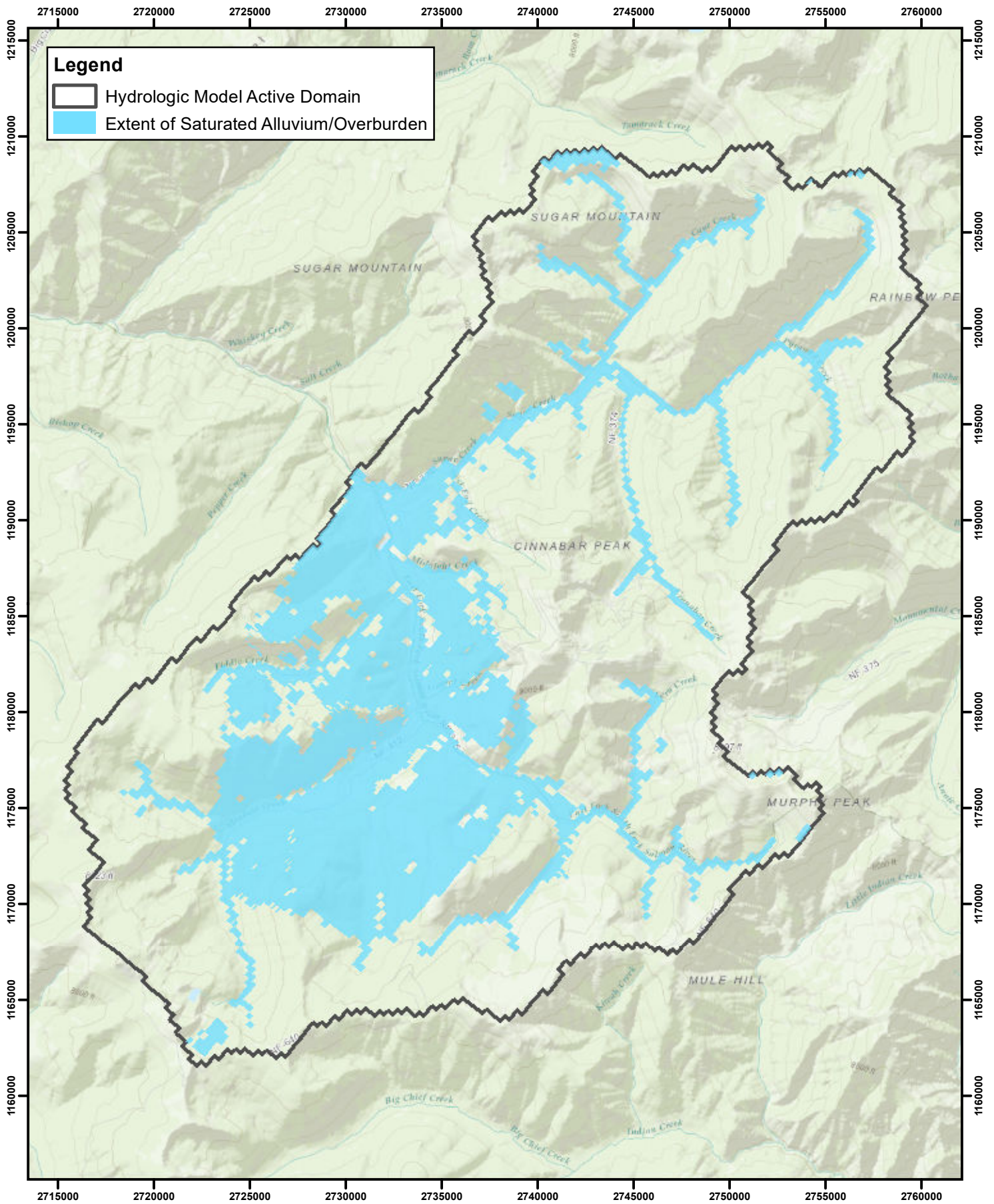


Figure 5-2
Simulated Extent of Saturated Alluvium and Overburden, February 2015
 Midas Gold Existing Conditions Model
 Stibnite Gold Project



Brown AND Caldwell

Date: November 10, 2017
 Project No: 150696
 Client: Midas Gold

Basemap:

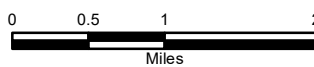


Figure 5-3
Simulated Extent of Saturated Alluvium
and Overburden, July 2015
 Midas Gold Existing Conditions Model
 Stibnite Gold Project

Stibnite Gold Project Modeling Process Overview

